Theory for Spin−Lattice Relaxation of Spin Probes on Weakly Deformable DNA

Alyssa L. Smith,[†] Pavol Cekan,[‡] David P. Rangel,[†] Snorri Th. Sigurdsson,[‡] Colin Mailer,[§] and Bruce H. Robinson*,[†]

Department of Chemistry, University of Washington, Seattle, Washington, Science Institute, University of Iceland, Reykjavik, Iceland, and Department of Radiology, University of Chicago, Chicago, Illinois

Received: November 26, 2007; Revised Manuscript Received: March 05, 2008

The weakly bending rod (WBR) model of double-stranded DNA (dsDNA) is adapted to analyze the internal dynamics of dsDNA as observed in electron paramagnetic resonance (EPR) measurements of the spin−lattice relaxation rate, R_{1e}, for spin probes rigidly attached to nucleic acid−bases. The WBR theory developed in this work models dsDNA base-pairs as diffusing rigid cylindrical discs connected by bending and twisting springs whose elastic force constants are κ and α, respectively. Angular correlation functions for both rotational displacement and velocity are developed in detail so as to compute values for R_{1e} due to four relaxation mechanisms: the chemical shift anisotropy (CSA), the electron−nuclear dipolar (END), the spin rotation (SR), and the generalized spin diffusion (GSD) relaxation processes. Measured spin−lattice relaxation rates in dsDNA under 50 bp in length are much faster than those calculated for the same DNAs modeled as rigid rods. The simplest way to account for this difference is by allowing for internal flexibility in models of DNA. Because of this discrepancy, we derive expressions for the spectral densities due to CSA, END, and SR mechanisms directly from a weakly bending rod model for DNA. Special emphasis in this development is given to the SR mechanism because of the lack of such detail in previous treatments. The theory developed in this paper provides a framework for computing relaxation rates from the WBR model to compare with magnetic resonance relaxation data and to ascertain the twisting and bending force constants that characterize DNA.

Introduction

The nature of internal motions in double-stranded DNA (dsDNA) is an ongoing area of nucleic acids research owing to the demonstrable importance of dynamics in explaining the mechanisms by which DNA functions.[1] In 1970, the time-resolved decay in the fluorescence polarization anisotropy (FPA) from ethidium intercalated between base-pairs revealed that DNA in solution is a flexible polymer that undergoes both about-axis twisting and bending.[2] To explain these data, Barkley and Zimm developed a continuous elastic model of internal Brownian twisting and bending motions of the double helix.[3] Concurrently, Allison and Schurr generated a theory for the twisting motion contribution to the FPA decay in which DNA is represented by a series of identical rigid rods connected by Hookean torsion springs.[4] This discrete model was subsequently extended by Schurr and co-workers to include bending motions for DNA modeled as spherical beads in a chain[5] coupled to nearest neighbors by a harmonic potential characterized by a torsion, α, and a bending, κ, elastic constant. This theory is referred to as the weakly bending rod (WBR) model. The discrete model provides a physical model with which to interpret the data from a variety of measurements on DNA. For example, the decay of the FPA from ethidium bromide intercalated in DNA is directly related to the mean square amplitudes and decay times for each of the normal modes of deformation[6–9] and hence the torsion elastic constant. Estimates of the dynamic persistence length are extracted from data obtained from a variety of measurements of DNA[5,9,10] using techniques that include transient polarization gratings,[11] transient photodichroism,[12] and electric birefringence.[13] The successes of the WBR model in explaining results from optical spectroscopy of dyes intercalated into DNA prompted Robinson and co-workers to apply a similar model to electron paramagnetic resonance (EPR) data from a spin-labeled intercalating probe.[14–16] In adapting the Schurr model, Robinson and co-workers combined both bending and twisting into a single unified model in which the base-pairs of DNA are modeled as cylinders whose geometry is characterized by the mean DNA hydrodynamic radius and average base-pair height for the B family conformations. These cylindrical subunits are connected by bending and twisting springs, also denoted by κ and α, respectively. The unified model offers simplicity at the expense of considering translational diffusion. However, translational diffusion is not measurable by EPR, and hence this sacrifice is not significant. In this paper, for simplicity, we will refer to this unified bending and twisting model as simply the WBR model.

In experiments using intercalators, there is little specific control over the distribution of dyes or probes along the DNA. Hence, measurements in such systems provide information on the average behavior of the duplex rather than site-specific data. In order to examine properties of duplex DNA as a function of sequence and position, great effort has been expended in developing probes that can be covalently bound to specific sites for use in EPR[10,17–23] and in labeling specific atoms by isotopic substitution to prepare sequences for NMR studies.[10,24–27]

EPR labeling experiments have focused on replacing natural bases with analogs, modified to contain the EPR active nitroxide radical as an integral part of the base. Early site-specific probes possessed large amplitudes of motion relative to the macromo-

* Corresponding author. E-mail: robinson@chem.washington.edu.
[†] University of Washington.
[‡] University of Iceland.
[§] University of Chicago.

10.1021/jp7111704 CCC: $40.75
Published on Web 07/02/2008

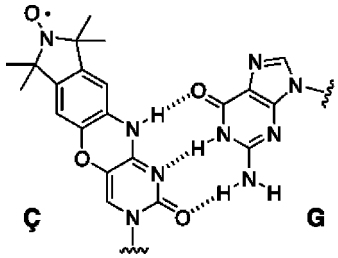

Figure 1. Rigid spin label Ç is shown base-paired to a natural guanine.[29]

lecular reference frame, as characterized by order parameters, S, falling below 0.4.[22,23] (The order parameter generally ranges from 0 to 1 with lower values indicating larger amplitudes of internal motions.) Subsequent efforts lead to the synthesis of more immobile probes as characterized by order parameters of 0.5, 0.8, and, more recently, 0.95.[19,20,28] In this paper, we present data using a recently developed spin probe, Ç ("C-spin"), that reports more faithfully on the DNA base motions to which it is rigidly locked.[29] The probe has a planar, rigid structure, rather than the single-bond tether common in nucleic acid spin probes (Figure 1). It has successfully been incorporated into a variety of nucleic acid sequences, and, in all cases, only nominally affects DNA duplex stability, presumably by effectively mimicking cytosine in its base-pairings.[29] Data supports the expectation that this probe is sensitive to the internal deformations of the DNA[10,29] and to processes with rotational correlations times as long as a microsecond.[30,31] These successes in syntheses have generated EPR spin probe data at specific base-pairs[21] in dsDNAs of lengths up to 50 base-pairs.

The WBR model has been applied in both EPR and NMR experiments on DNA to uniquely distinguish between tumbling and rapid internal motions.[10,21,27,32–35] Continuous wave (CW) EPR has been used in our laboratory to characterize the internal motions of DNA and RNA, and we have reported bending force constants and have shown that the persistence length determined from early time bending dynamics is about two- to threefold larger than that from long time-scale motions.[21] This result is important because it demonstrates that the bending of DNA must ultimately be described by an internal potential that responds to different length scales within the duplex DNA.

While CW-EPR has provided valuable insight into the nature of the internal dynamics of nucleic acids, it is primarily sensitive to motional processes that are fast enough to compete with the rapid spin−spin dephasing rate, R_{2e}. In contrast, pulsed saturation recovery (pSR) EPR measures processes that compete with the spin−lattice recovery rate, R_{1e}, and hence affords a window into slower motions that characterize collective internal deformations of the DNA filament. The R_{1e} is particularly sensitive to motional processes, with a characteristic relaxation time, τ, on the order of $\omega\,\tau \approx 1$, where ω is the spectrometer frequency. In the case of EPR, the spectrometer frequency is generally between 1 and 35 GHz. The WBR theory predicts that the time constant, τ, for internal motions of DNA are on the subnanosecond scale and therefore ideally suited to be detected by spectrometers in the 1 to 10 GHz range, making this a technique well-suited to measure internal motion in nucleic acids. We have previously demonstrated that pSR measurements on DNA are experimentally possible,[36] but here we report the first detailed measurements of R_{1e} on a series of dsDNA. This R_{1e} data serve as the motivation for the present effort to further develop and extend the WBR model to make predictions for site-specific dynamics. The model for calculating R_{1e} based on a rigid rod-like molecule is shown to be insufficient to explain the data. The discrepancy between a simple motional model (previously developed[37]) and the data we present here is compelling motivation to develop an analysis of the pSR DNA spin−lattice relaxation rates, in terms of the WBR model, which allows for internal twist and flexure.

As further impetus to pursue pSR EPR, we turn to other work in which this technique has been successfully applied to biological systems to measure the solvent accessibility of spin-labeled residues on membrane proteins and to observe the properties of lipid membranes.[36,38–44] There is a precedent for the usefulness of pSR experiments in the study of dynamics; Hubbell has suggested that if the R_{1e} internal dynamic modes are known at particular sites on a protein, then, for example, the local backbone fluctuations can be ascertained.[45]

R_{1e} rates are produced by four mechanisms. The largest of these, in most cases, is the electron−nuclear dipolar (END) coupling between the nitroxide electron and the nitrogen (^{14}N) nucleus.[37] The other three mechanisms are spin rotation (SR), chemical shift anisotropy (CSA), and generalized spin diffusion (GSD). We have described previously how the dynamics of an anisotropically tumbling rigid rod-like molecule can be incorporated into the expressions for the electron spin−lattice relaxation rate[37] and have shown how the diffusive dynamics of this simple model can be obtained from fitting these equations to pSR EPR data.[44,45] The current work endeavors to incorporate the more elaborate rotational displacement and velocity correlation functions into the various spin−lattice mechanisms so as to produce expressions for R_{1e} rates based on the WBR model. In doing so, we provide a computational method to extract information on the dynamics of DNA from relaxation data. Specifically, we adapt the WBR model so that it can be used to generate rotational position and velocity correlation functions to insert into R_{1e} rate mechanisms. Special attention is given to the spin−rotation mechanism for it requires a new expression for the angular velocity autocorrelation function. This correlation function has not been presented in the literature and is one of our main contributions in this work.

EPR[22,23,46] and NMR[35,47–49] relaxation data have been characterized by use of the Lipari−Szabo (L−S) model-free approach.[50] The goal of the model-free approach is to determine the order parameters and internal correlation times from experimental line widths and relaxation data.[47] However, CW-EPR data cannot be directly analyzed by the L−S approach, because the spectra are sensitive to dynamics that broaden the lines beyond the limits of applicability of the L−S method.[50,51] The R_{1e} experimental data obtained by pSR, on the other hand, can be modeled by the L−S approach, as will be demonstrated in this work. We shall identify the correspondence between the correlation functions derived under the WBR model with the parameters in the L−S model. In doing so, we lend physical meaning to model-free L−S order parameters by linking these to the model-dependent WBR theory. The result is a data analysis scheme that is a hybrid between the two approaches. It combines the simplicity of the L−S method with the substantive predictions made by the WBR model. We will show that the WBR model can be used to determine the dependence of the order parameters on label position, bending force constants, and length of the DNA.

The WBR model predicts that the decay of the autocorrelation functions of the internal modes at different time regimes have varied power law dependencies.[4,52] We take advantage of that by using stretched exponentials to model the autocorrelation functions obtained from the WBR model. We will develop the

appropriate correlation functions in terms of the WBR model and demonstrate how to obtain the spectral density functions from the Fourier transform of a stretched exponential. This will provide a basis for including the internal dynamics of the WBR model in the analysis of R_{1e}.[53–57]

Our goal in this paper is to demonstrate that experimental R_{1e} rates contain information on the internal motions of DNA and that the WBR model can be adapted to analyze those motions in terms of the twisting and bending force constants. We develop spectral density functions required to analyze the dynamics. The methods developed here will provide a practical framework to relate experimental data to internal modes of motion in biopolymers.

Theory

1. Spin−Lattice Relaxation. We have demonstrated previously that the principal mechanisms responsible for anisotropically driven spin−lattice relaxation can be well-understood in the liquids regime using the formalism of the Redfield theory.[37] Previous work in this laboratory has developed the theoretical framework in which the dominant Hamiltonians of nitroxide-based EPR probes are used to obtain expressions for R_{1e}.[37,58] In this theory, the Redfield spin−lattice relaxation rate is directly related to stochastically fluctuating, nonsecular EPR Hamiltonians:

$$R_{1e} = \int_{\tau=0}^{\infty} \mathrm{trace}\left\{[O_z, \overline{H'(0)], [\widetilde{H'}(\tau), O_z^{\dagger}]}\right\} \mathrm{d}\tau \quad (1.1)$$

where H' is a perturbation Hamiltonian that consists of the spin operators and a fluctuating lattice contribution, usually in a form that is bilinear in spin and lattice variables. $O_z \propto S_z$ is the operator associated with the electron spin−lattice relaxation and satisfies the requirement that trace$\{O_z^{\dagger}O_z\} = 1$. The Hamiltonian, H', in eq 1.1 is the sum of the Hamiltonians for each of the four mechanisms introduced below. Theses four mechanisms are the electron−nuclear dipolar (END), chemical shift anisotropy (CSA), spin rotation (SR), and generalized spin diffusion (GSD). The rates associated with each of the four mechanisms, at the level of approximation embodied in eq 1.1, add independently to give the total spin−lattice relaxation rate:

$$R_{1e} = R_{1e}^{\mathrm{END}} + R_{1e}^{\mathrm{CSA}} + R_{1e}^{\mathrm{SR}} + R_{1e}^{\mathrm{GSD}} \quad (1.2)$$

The electron−nuclear dipolar (END) term encompasses the magnetic dipole−dipole interaction between the electron spin and the local nuclei, while the chemical shift anisotropy (CSA) is due to anisotropy in the coupling between the electron spins to the applied, external magnetic field. Both the END and the CSA interactions depend upon the orientation of the spin label. The cross correlation between the END and the CSA Hamiltonians has been developed elsewhere[58] but is neglected here for simplicity. The spin rotation (SR) relaxation arises from a coupling between the magnetic moment of the electron spin and the angular velocity of the spin probe with respect to the external fixed reference frame. Utilizing a relaxation rate formalism previously developed for rigid rod-like lipids,[37] we will, in the following sections, provide explicit expressions for these first three mechanisms in terms of the rotational dynamics of DNA modeled by the WBR theory. The final rate is due to generalized spin diffusion (GSD) relaxation. GSD provides an important contribution to R_{1e}, especially at X-band frequencies, and must be considered in any practical analysis of the actual relaxation rates observed in experimental work. Unfortunately, at the present, a definitive connection between the observed diffusion of the probe magnetization to the surrounding spins and molecular dynamics is not well-established. We therefore provide a functional form of this mechanism in terms of a generic effective diffusion time that accounts for the data but fails to provide a direct connection to the dynamics of DNA, the probe, and the local environment.

We begin with a discussion of the general form for each term of the relaxation rate. This provides a framework into which any model for the dynamics of the system can be inserted. We then derive expressions for the dynamics of the system in terms of spectral densities of the autocorrelations for rotational displacement and velocity. We emphasize spin rotation as it is often neglected and, as such, has an underdeveloped theory. Following this general introduction, we develop in detail the rotational autocorrelation functions for the WBR model that are applicable to pSR data from site-specifically labeled DNA and, in doing so, present a novel development of the SR spectral density functions using the angular velocity correlation functions appropriate for internal deformations. We then demonstrate how the L−S method of analysis can be adapted to place the WBR results in terms of the common parameters that appear in the model-free approach. A benefit of the correspondence we establish between the modified L−S method and the WBR model results is a computationally tractable framework for analysis of EPR data. We provide an explicit example of how this is done for the SR mechanism to conclude the theory section.

1.A. Electron−Nuclear Dipolar Interaction. The END mechanism is the electron analogy to dipolar relaxation in NMR. The relaxation rate, computed from the spectral density functions, is found in many treatments[37] and standard texts:[59]

$$R_{1e}^{\mathrm{END}} = \frac{2}{9} I(I+1) \sum_{p,p'=-2}^{2} W_{p,p'}^{\mathrm{END}} \boldsymbol{R}(J_{p,p'}(\omega_e)) \quad (1.3)$$

The rate of relaxation is proportional to the real part of the spectral density function, $J_{p,p'}(\omega_e)$, which is the one-sided Fourier transform of the position correlation function:

$$J_{p,p'}(\omega_e) = \int_{\tau=0}^{\infty} G_{p,p'}(\tau)\, \mathrm{e}^{-i\omega_e \tau}\, \mathrm{d}\tau \quad (1.4)$$

where $G(\tau)$ is the angular displacement correlation function. Because the EPR pSR experiment measures the rate of the relaxation of the electron, the spectral density function is evaluated only at the spectrometer frequency, $\omega = \omega_e$. $G(\tau)$ is expressed in terms of the ensemble average of the correlation function between elements, Dp,q^2, of the Wigner rotation matrix (WRM), $\mathbf{D}^2$:

$$G_{p,p'}(\tau) = \delta_{q,q'} \left\langle D_{p',q'}^{2*}(\Omega(\tau)) D_{p,q}^{2}(\Omega(0)) \right\rangle \quad (1.5)$$

This position correlation function is independent of the value of the indices (q and q') which are associated with the angle γ in the Euler rotation sequence, $\Omega = (\alpha, \beta, \gamma)$, that carries the END coupling tensor, $\mathbf{a} = \mathbf{A} - \bar{a}\mathbf{1}$, from the laboratory to the principal axis frame in which $\mathbf{a}$ is diagonal. $\mathbf{A}$ is the hyperfine tensor, and $\bar{a} = \mathrm{trace}\{\mathbf{A}\}/3$. Subtraction of $\bar{a}$ removes the contact term between the electron and the nucleus and leaves the dipolar part of $\mathbf{A}$ in the END Hamiltonian. The principal axis frame, in which $\mathbf{a}$ is diagonal, is stationary in the molecular frame to the extent to which the probe is rigidly attached. As such, R_{1e}^{END} is a measure of internal deformations of the macromolecule, as well as its anisotropic rigid-body spinning or end-over-end tumbling, otherwise referred to as the uniform modes of rotation. The principal axis frame (PAS), A, of $\mathbf{a}$ will not in general be coincident with the molecular frame, D, in which the local

diffusion tensor is diagonal. The matrix, $\mathbf{W}^{\mathrm{END}}$, allows for a static rotation $\Omega_{\text{D-A}}$ between these two frames:

$$\mathbf{W}^{\mathrm{END}} = \mathbf{D}^{2\dagger}(\Omega_{\mathrm{D-A}})(\alpha\alpha^{\dagger})\mathbf{D}^{2}(\Omega_{\mathrm{D-A}}) \tag{1.6}$$

where $\alpha^{\dagger} \equiv (\alpha_2\ \alpha_1\ \alpha_0\ \alpha_{-1}\ \alpha_{-2}) = \sqrt{5}[a_-\ 0\ \sqrt{2/3}(a_+ - a_{zz})\ 0\ a_-]$ and $\alpha_{\pm} = (\alpha_{yy} \pm \alpha_{xx})/2$. The elements a_{xx}, a_{yy}, and a_{zz} are the diagonal components of **a** that is diagonal in the A frame.

1.B. Chemical Shift Anisotropy. The CSA relaxation mechanism is of a form similar to that of the END:

$$R_{1\mathrm{e}}^{\mathrm{CSA}} = \frac{1}{5}\sum_{p,p'=-2}^{2} W_{p,p'}^{\mathrm{CSA}}\boldsymbol{R}(J_{p,p'}(\omega_e)) \tag{1.7}$$

The spectral density, $J_{p,p'}(\omega_e)$, is the same as that used to evaluate the END relaxation rate given in eq 1.4. Here, the coupling takes place between the electron spin and the magnetic field, $\mathbf{H} = H\hat{z}$, oriented by $\hat{z}$, which is a unit vector in the laboratory z direction, via the anisotropic CSA tensor, **G**. The magnitude of the field, H, is related to the spectrometer frequency, ω_e, by $\omega_e = \bar{g}(\beta_e/\hbar)H$, where β_e is the Bohr magnetron and $\bar{g} = (1/3)\mathrm{trace}\{\mathbf{G}\}$. Ordinarily, the isotropic part of **G** is removed from the Hamiltonian as it plays no part in longitudinal relaxation. The remaining anisotropic CSA tensor is denoted by $\mathbf{g} \equiv \mathbf{G} - \bar{g}\mathbf{1}$. In the CSA principal axis frame, G, this tensor is given by

$$\mathbf{g} = \begin{pmatrix} g_{xx} & 0 & 0 \\ 0 & g_{yy} & 0 \\ 0 & 0 & g_{zz} \end{pmatrix} \tag{1.8}$$

The transformation matrix $\mathbf{W}^{\mathrm{CSA}}$ has the same form as $\mathbf{W}^{\mathrm{END}}$ in eq 1.6. The variables in eq 1.7) are again expressible in terms of the WRM functions:

$$\mathbf{W}^{\mathrm{CSA}} = \mathbf{D}^{2\dagger}(\Omega_{\mathrm{D-G}})(\gamma\gamma^{\dagger})\mathbf{D}^{2}(\Omega_{\mathrm{D-G}}) \tag{1.9}$$

where $\gamma^{\dagger} = (\omega_e\sqrt{5}/\bar{g})(g_-\ 0\ \sqrt{2/3}(g_+ - g_{zz})\ 0\ g_-)$, $g_{\pm} = (g_{yy} \pm g_{xx})/2$, and $\Omega_{\text{D-G}}$ is the rotation from the CSA principal axis frame, G, to the molecular frame, D, in which the diffusion tensor is diagonal.

1.C. Spin Rotation. Unlike CSA and END relaxation mechanisms, spin rotation (SR) has received only minimal attention in the literature.[60–63] For this reason, we shall spend more time here to describe in detail the SR Hamiltonian and relaxation rate.

The SR Hamiltonian is given by[64]

$$H^{\mathrm{SR}} = -\mathbf{SR}(\Omega_{\mathrm{L-D}}(t))\mathbf{R}(\Omega_{\mathrm{D-G}})(\mathbf{G} - g_{\mathrm{free}}\mathbf{1})\mathbf{R}(\Omega_{\mathrm{D-G}})\mathbf{R}(\Omega_{\mathrm{I-D}})\omega_{\mathrm{I}}(t) \tag{1.10}$$

where $\boldsymbol{\omega}_{\mathrm{I}}$ is the angular velocity in Cartesian coordinates of the nitroxide in the principal axis frame, I, of the molecular inertial tensor, **I**. **S** is the electron spin operator in the laboratory-fixed frame, L, and is also expressed in Cartesian coordinates. **G** is the CSA full coupling tensor, and $g_{\mathrm{free}} = 2.0023$ is the g factor of the free electron. The rotation matrixes that connect the reference frames of $\boldsymbol{\omega}_{\mathrm{I}}$, **G**, and **S** are inserted between each of these in eq 1.10 and are all time-independent, with the exception of $\mathbf{R}(\Omega_{\text{L-D}}(t))$. Analytic expression for angular displacement correlation functions involving this rotation matrix that are needed to calculate $R_{1\mathrm{e}}^{\mathrm{SR}}$, are more easily formulated in a spherical basis set. This transformation from rectilinear to spherical coordinates is accomplished through use of the matrix operator, **U**:

$$\mathbf{U} = \frac{1}{\sqrt{2}}\begin{pmatrix} 1 & -i & 0 \\ 0 & 0 & \sqrt{2} \\ -1 & -i & 0 \end{pmatrix} \tag{1.11}$$

The transformation, **U**, converts the Cartesian spin variables labeled x, y, and z to their spherical counterparts labeled −1, 0, and 1. The Cartesian spin operator is denoted by **S** and its spherical counterpart by S. **U** also converts the Cartesian rotation matrix into a first rank WRM, $\mathbf{D}$.[1] For simplicity, we assume here that the I frame is coincident with the PAS of the molecular diffusion tensor, or D frame, so that $\mathbf{R}(\Omega_{\text{I-D}}) = \mathbf{1}$. By implementing these transformations, eq 1.10 can be rewritten as

$$H^{\mathrm{SR}} = -\boldsymbol{S}^{\dagger}\mathbf{D}^{1\dagger}(\Omega_{\mathrm{L-D}}(t))\boldsymbol{g}\omega_{\mathrm{I}}(t) \tag{1.12}$$

where $\boldsymbol{g} = \mathbf{U}\mathbf{R}^{-1}(\Omega_{\text{D-G}})\cdot(\mathbf{G} - g_{\mathrm{free}}\mathbf{1})\mathbf{R}(\Omega_{\text{D-G}})$ Note that although $\boldsymbol{g}$ is non-Hermitian, the overall Hamiltonian remains self-adjoint. Equation 1.12 is now used to compute $R_{1\mathrm{e}}^{\mathrm{SR}}$ as instructed by the Redfield approximation in eq 1.1. As this computation has been performed elsewhere, we now summarize the results that ensue.[37]

$R_{1\mathrm{e}}^{\mathrm{SR}}$ retains the form of a product between a time-independent matrix, $\mathbf{W}^{\mathrm{SR}}$, that accounts for the fixed I to D and D to G frame rotations, and a spectral density function, $\mathbf{J}^{\mathrm{SR}}$:

$$R_{1\mathrm{e}}^{\mathrm{SR}} = 2\sum_{p,p'=-1}^{1}\sum_{m,m'=1}^{3} W^{\mathrm{SR}m,m'}_{p,p'}\boldsymbol{R}(J^{\mathrm{SR}m,m'}_{p,p'}(\omega_e)) \tag{1.13}$$

The m index refers to the Cartesian components (x, y, and z) of the angular velocity, and the p index (−1, 0, and 1) identifies the spherical components of the WRM elements. The components of the time-independent matrix $\mathbf{W}^{\mathrm{SR}}$ is related to products of g matrix elements:

$$W^{\mathrm{SR}m,m'}_{p,p'} = \boldsymbol{g}^{*}_{p',m'}\boldsymbol{g}_{p,m} \tag{1.14}$$

The spectral density function for spin rotation is:

$$J^{\mathrm{SR}m,m'}_{p,p'}(\omega_e) = \int_{\tau=0}^{\infty} G^{\mathrm{SR}m,m'}_{p,p'}(\tau)\,\mathrm{e}^{-i\omega_e\tau}\,\mathrm{d}\tau \tag{1.15}$$

The correlation function for spin rotation, $G^{\mathrm{SR}m,m'}_{p,p'}(\tau)$, that appears in eq 1.15 contains both the autocorrelation of rotational displacement and the angular velocity:[61,63]

$$G^{\mathrm{SR}m,m'}_{p,p'}(\tau) = \delta_{n,n'}\langle D^{1*}(\Omega_{\mathrm{L-D}}(0))_{p,n}D^{1}(\Omega_{\mathrm{L-D}}(\tau))_{p',n'}(\omega_{\mathrm{I}}(0)\omega_{\mathrm{I}}^{\dagger}(\tau))_{m,m'}\rangle \tag{1.16}$$

The fact that the angular velocity correlation functions are evaluated in the molecular inertial tensor PAS, I, (or, equivalently, the diffusion tensor PAS, D, under our assumption above) leads to the correlation functions requiring only first rank instead of second rank WRMs that appear in the END and CSA relaxation mechanisms.

A reasonable assumption that the angular velocity correlation functions are statistically independent of the reorientation correlation functions allows separate ensemble averaging of the position and velocity correlation functions:[37,61]

$$G^{\mathrm{SR}m,m'}_{p,p'}(\tau) = \delta_{n,n'}\langle D^{1*}(\Omega_{\mathrm{L-D}}(0))_{p,n}D^{1}(\Omega_{\mathrm{L-D}}(\tau))_{p',n'}\rangle \times \langle(\omega_{\mathrm{I}}(0)\omega_{\mathrm{I}}^{\dagger}(\tau))_{m,m'}\rangle \tag{1.17}$$

Development of the correlation functions for the angular velocity correlation functions has been performed for rigid

anisotropically diffusing bodies previously.[37] In section 2, below, we present a detailed derivation of angular velocity correlation functions specific to internal motion in DNA as idealized in the WBR model.

1.D. Generalized Spin Diffusion (GSD). We conclude part 1 of Theory with a generalization of the spin diffusion processes (GSD) that is discussed most frequently in the context of NMR,[17,65] but is equally important for electron relaxation.[37,66] Because GSD involves diffusion of magnetization among spins, there is only an indirect connection with the molecular motions of the system. Therefore, for the present, this mechanism remains a constant for all nitroxide spin systems. There is, however, a fundamental connection between the spin diffusion and the diffusive processes that drive the molecular system. In general, there is diffusion of the solvent nuclear polarization in the network of the surrounding solvent protons by nuclear dipole−dipole "flip-flops". The proton−proton spin flip-flop transition rate occurs on a 10 ps time scale for water at around 20 °C.[59] The form of the relaxation rate for this spin-diffusion mechanism[66] adapts de Gennes's theory of spin-diffusion to the case of electron relaxation.[67]

$$R_{1e}^{GSD} = R_{1e,max}^{SD}\left(\frac{2w_x\tau_d}{1+(\omega_e\tau_d)^{3/2}}\right)^{1/4} \tag{1.18}$$

τ_d is the relative solvent-nitroxide translational diffusion time, and $R_{1e,max}^{SD} = 0.15$ Mrad/s at X-band frequencies. w_x is the X-band reference frequency: $w_x = 2\pi \times 9.3$ GHz.[66] When $\omega_e\tau_d = 1$ and the spectrometer resonance frequency is 9.3 GHz, $R_{1e}^{GSD} = 0.15$ Mrad/s.[37]

Having summarized the four mechanisms that contribute significantly to nitroxide spin−lattice relaxation, we now turn to the evaluation of spectral density functions for the WBR model of dynamics of DNA.

2. WBR Model for DNA Internal Dynamics. We will briefly review the dynamics of the WBR model that is described in greater detail elsewhere.[21,52,68] Our focus in this paper is to develop velocity autocorrelation functions for the WBR model that are applicable to the SD relaxation mechanism. We will begin the discussion of the WBR model by summarizing the results for twisting motions. We then show how the methods used in deriving the twisting correlation functions can be extended to deal with the more complicated bending dynamics.

2.A. Twisting. Twisting of the N discs in the WBR model is governed by the Langevin equation. The twist of each disk relative to the equilibrium position is indicated by the angle ϕ_i. Each disk has the same moment of inertia, I, for the rotation about the axis of symmetry, and a friction factor, γ, that accounts for viscous drag. $N - 1$ equivalent Hookean twisting springs with spring constant, α, between neighboring discs produce restoring torques that define the lowest energy state of the WBR. The effects of the solvent are modeled by Gaussian random torques, $\Gamma_i(t)$. The Langevin equation for twisting is expressible for the ith disk in terms of these variables:

$$I\ddot{\phi}_i(t) + \gamma\dot{\varphi}_i(t) + \alpha\{\varphi_{i+1}(t) - \varphi_i(t)\} + \alpha\{\varphi_{i-1}(t) - \varphi_i(t)\} = \Gamma_i(t) \tag{2.1}$$

The N Langevin equations for all discs in the WBR can be written together in terms of a matrix equation:

$$I\ddot{\boldsymbol{\varphi}}(t) + \gamma\dot{\boldsymbol{\varphi}}(t) + \alpha\mathbf{A}\boldsymbol{\varphi}(t) = \Gamma(t) \tag{2.2}$$

where

$$\boldsymbol{\varphi}(t) = \begin{pmatrix}\varphi_1(t)\\ \vdots \\ \varphi_N(t)\end{pmatrix} \tag{2.3}$$

and

$$\mathbf{A} = \begin{pmatrix}-1 & 1 & 0\\ 1 & -2 & 1\\ 0 & 1 & \ddots\end{pmatrix} \tag{2.4}$$

where $\mathbf{A}$ here is not to be confused with the END coupling tensor.

The total potential energy for the twisting, U, can be written in terms of $\mathbf{A}$:

$$U = \frac{1}{2}\alpha\boldsymbol{\varphi}^{\dagger}\mathbf{A}\boldsymbol{\varphi} \tag{2.5}$$

The $\mathbf{A}$ matrix contains all of the nearest-neighbor interactions but none of the adjustable constants. It is a tridiagonal real and symmetric matrix.[5] As such, $\mathbf{A}$ may be diagonalized by an orthogonal transformation, $\mathbf{Q}$ for which $\mathbf{Q}^{\dagger}\mathbf{Q} = \mathbf{1}$. The transformation matrix, $\mathbf{Q}$, like $\mathbf{A}$, depends only on the number of discs comprising the DNA and produces the diagonal eigenmatrix, $\boldsymbol{\Lambda}$, comprised of the eigenvalues of $\mathbf{A}$:

$$\mathbf{Q}^{\dagger}\mathbf{A}\mathbf{Q} = \Lambda \tag{2.6}$$

Formally, the inverse of $\mathbf{A}$ is given by

$$\mathbf{A}^{-1} = \mathbf{Q}\Lambda^{-1}\mathbf{Q}^{\dagger} \tag{2.7}$$

However, $\boldsymbol{\Lambda}$ contains a single zero eigenvalue, which physically represents the rotation of the entire molecule, more commonly referred to as the uniform mode. Therefore, the inverse in eq 2.7 is not well-defined. Because the analysis to follow requires this inverse for the nonzero eigenvalues, $\mathbf{A}^{-1}$ is computed with the zero eigenvalue in $\boldsymbol{\Lambda}$, and the associated eigenvector in $\mathbf{Q}$ is removed. This form of the inverse is called the principal inverse or pseudoinverse. The removal of the equation associated with the zero eigenvalue has been carefully developed by Schurr and co-workers.[5]

The equation of motion can now be written in terms of uncoupled normal twisting modes, represented here by the vector $\boldsymbol{\rho}$ of length N:

$$I\ddot{\rho}(t) + \gamma\dot{\rho}(t) + \alpha\Lambda\rho(t) = \mathbf{Q}^{\dagger}\Gamma(t) \tag{2.8}$$

where the relationship between the normal modes and twist angle is given by:

$$\boldsymbol{\varphi}(t) = \mathbf{Q}\rho(t) \tag{2.9}$$

Equation 2.8 is solved to determine the twisting autocorrelation functions for the normal modes:

$$\mathbf{C}_{\rho}(t) \equiv \langle\rho(0)\rho^{\dagger}(t)\rangle \tag{2.10}$$

The normal mode correlation functions are then transformed with the matrix $\mathbf{Q}$ to produce the desired twist angle correlation matrix:

$$\mathbf{C}(t) \equiv \langle\boldsymbol{\varphi}(0)\boldsymbol{\varphi}(t)\rangle = \mathbf{Q}\mathbf{C}_{\rho}(t)\mathbf{Q}^{\dagger} \tag{2.11}$$

$\mathbf{C}(t)$ contains all possible N^2 position auto- and cross-correlation functions. The corresponding twisting velocity correlation functions for the normal modes are denoted by

$$\mathbf{V}_{\rho}(t) \equiv \langle\dot{\rho}(0)\dot{\rho}(t)\rangle \tag{2.12}$$

and are used to provide an expression for the auto- and cross-correlation twisting angle velocity matrix:

$$\mathbf{V}(t) \equiv \langle \dot{\boldsymbol{\varphi}}(0)\dot{\boldsymbol{\varphi}}(t)\rangle = \mathbf{Q}\mathbf{V}_{\rho}(t)\mathbf{Q}^{\dagger} \tag{2.13}$$

Equations 2.8 and 2.10 are combined to produce N independent second order ordinary differential equations. Since the random torques are uncorrelated with the velocity and position of ith modes, these differential equations take the following form:

$$I\ddot{C}_{\rho_i}(t) + \gamma\dot{C}_{\rho_i}(t) + \alpha\Lambda_i C_{\rho_i}(t) = 0 \tag{2.14}$$

The solution to this differential equation is

$$C_{\rho_i}(t) = \frac{kT}{2\alpha\Lambda_i}\left\{\left(1 - \frac{1}{S_i}\right)\mathrm{e}^{-r_{i+}t} + \left(1 + \frac{1}{S_i}\right)\mathrm{e}^{-r_{i-}t}\right\} \tag{2.15}$$

where

$$r_{i\pm} = \frac{\gamma}{2I}\{1 \pm S_i\} \tag{2.16}$$

and

$$S_i = \sqrt{1 - \frac{4I\Lambda_i\alpha}{\gamma^2}} \tag{2.17}$$

The results for all N modes are combined in matrix equation form, and the transformation matrix $\mathbf{Q}$ is used to obtain the correlation matrix for the angular displacements, $\mathbf{C}(t)$:

$$\mathbf{C}(t) = \mathbf{Q}\mathbf{C}_{\rho}(t)\mathbf{Q}^{\dagger}$$

$$= \frac{kT}{2\alpha}\mathbf{Q}\boldsymbol{\Lambda}^{-1}\mathbf{S}^{-1}\{(\mathbf{S} - 1)\,\mathrm{e}^{-\mathbf{r}_{+}t} + (\mathbf{S} + 1)\,\mathrm{e}^{-\mathbf{r}_{-}t}\}\mathbf{Q}^{\dagger} \tag{2.18}$$

where

$$\mathbf{r}_{\pm} = \frac{\gamma}{I}\frac{\{1 \pm \mathbf{S}\}}{2} \tag{2.19}$$

and

$$\mathbf{S} = \sqrt{1 - 4\Lambda\frac{(\alpha/\gamma)}{(\gamma/I)}} \tag{2.20}$$

Notice that the amplitude in eq 2.15 diverges for the $i = 1$, or uniform mode, for which $\Lambda_1 = 0$. The uniform mode, $\rho_1(t)$, and its associated correlation function, $C_{\rho_1}(t)$, must be treated differently. In this case, the amplitude is derived from the "difference" displacement correlation function, $\delta C_{\rho_1}(t) = \langle(\rho_1(t) - \rho_1(0))^2\rangle$, which can be shown[52] to have the property that

$$\langle(\rho_1(t) - \rho_1(0))^2\rangle = 2\frac{kT}{\gamma}t \tag{2.21}$$

Unlike the uniform mode, the internal mode amplitudes are derived from the equilibrium requirement on the $C_{\rho_i}(t)$; that is,

$$\langle\rho_i(t)\rho_j(t)\rangle = \langle\rho_i^2(0)\rangle$$

$$= \frac{kT}{\Lambda_i\alpha} \tag{2.22}$$

where the first equality derives from the fact that the normal modes are uncoupled and from the fact that the diffusive process is assumed to be a stationary process. The entire set of internal correlation functions amplitudes can be written in a compact matrix form:

$$\mathbf{C}(0) = \langle\varphi(0)\varphi^{\dagger}(0)\rangle$$

$$= \langle\varphi(t)\varphi^{\dagger}(t)\rangle$$

$$= \frac{kT}{\alpha}\mathbf{Q}\boldsymbol{\Lambda}^{-1}\mathbf{Q}^{\dagger}$$

$$= \frac{kT}{\alpha}\mathbf{A}^{-1} \tag{2.23}$$

where the uniform mode has been excluded from the inverse and is treated separately, as discussed above.

Also note that in the over damped regime, which is the limit in which treatments in the literature commonly operate, $\mathbf{C}(t)$ is found by letting the moment of inertia go to zero:

$$\lim_{I\to 0}\mathbf{C}(t) \to \frac{kT}{\alpha}\mathbf{Q}\boldsymbol{\Lambda}^{-1}e^{-\frac{a}{\gamma}\boldsymbol{\Lambda}t}\mathbf{Q}^{\dagger} = \frac{kT}{\alpha}\mathbf{A}^{-1}e^{-\frac{a}{\gamma}\mathbf{A}t} \tag{2.24}$$

The normal mode velocity autocorrelation functions are most directly derived using the following relation:

$$V_{\rho_i}(t) \equiv \langle\dot{\rho}_i(0)\dot{\rho}_i(t)\rangle$$

$$= -\langle\rho_i(0)\ddot{\rho}_i(t)\rangle$$

$$= -\frac{d^2C_{\rho_i}(t)}{dt^2} \tag{2.25}$$

This relationship is derived as follows. Note first that

$$\frac{\partial\langle\rho_i(x)\rho_i(t+x)\rangle}{\partial x} = 0 \tag{2.26}$$

because $C_{\rho_i}(t)$ describes a stationary Markov process and is therefore independent of the starting time, x. Then

$$\frac{\partial\langle\rho_i(x)\rho_i(t+x)\rangle}{\partial x} = \langle\dot{\rho}_i(x)\rho_i(t+x)\rangle + \langle\rho_i(x)\dot{\rho}_i(t+x)\rangle$$

$$= 0 \tag{2.27}$$

so that, when $x = 0$, we obtain

$$\langle\dot{\rho}_i(0)\rho_i(t)\rangle = -\langle\rho_i(0)\dot{\rho}_i(t)\rangle$$

$$\equiv -\frac{\mathrm{d}C_{\rho_i}(t)}{\mathrm{d}t} \tag{2.28}$$

In a parallel fashion, we can get the relation among higher derivatives

$$\frac{\partial\langle\rho_i(x)\dot{\rho}_i(t+x)\rangle}{\partial x} = \langle\dot{\rho}(x)\dot{\rho}(t+x)\rangle + \langle\rho(x)\ddot{\rho}(t+x)\rangle$$

$$= 0 \tag{2.29}$$

and set $x = 0$ to arrive at eq 2.25. Equation 2.25 permits us to use our results from the normal mode displacement correlation function to directly compute $V_{\rho_i}(t)$ by simply taking two derivatives of the expression in eq 2.15. We obtain as a solution

$$V_{\rho_i}(t) = \frac{kT}{I}\frac{1}{2S_i}\{(1 + S_i)\,\mathrm{e}^{-r_{i+}t} - (1 - S_i)\,\mathrm{e}^{-r_{i-}t}\} \tag{2.30}$$

Unlike the position autocorrelation function, note that the velocity autocorrelation function for the uniform mode is well-behaved for the uniform mode in which $\Lambda_1 = 0$:

$$V_{\rho_1}(t) = \frac{kT}{I}\,\mathrm{e}^{-\frac{\gamma}{I}t} \tag{2.31}$$

It is important to note that eq 2.31 is precisely the autocorrelation function obtained for a single disk of moment of inertia, I, and friction factor, γ.[69]

We again use a matrix equation to succinctly express the set of all velocity correlation functions:

$$\mathbf{V}(t) = \mathbf{Q}\mathbf{V}_\rho(t)\mathbf{Q}^\dagger$$

$$= \frac{kT}{I}\mathbf{Q}\frac{\mathbf{S}^{-1}}{2}\{(1+\mathbf{S})\,\mathrm{e}^{-\mathbf{r}_+t} - (1-\mathbf{S})\,\mathrm{e}^{-\mathbf{r}_-t}\}\mathbf{Q}^\dagger \tag{2.32}$$

Since $\mathbf{r}_\pm$ and $\mathbf{S}$ are diagonal, $\mathbf{V}_\rho(t)$ matrix is also diagonal. The initial velocity autocorrelation is the same for each mode, including the first, or uniform, mode, and is given by

$$\mathbf{V}(0) = \frac{kT}{I}\mathbf{1} \tag{2.33}$$

where $\mathbf{1}$ is the N by N identity matrix.

An important consequence of the fluctuation−dissipation theorem is that the diffusion coefficient is the integral of the velocity autocorrelation function. Hence, the diffusion of a single disk, D_{disk}, is a functional of the velocity autocorrelation of the single disk,[69] which, in turn, is an integral over the uniform mode result, eq 2.31, by virtue of the indistinguishability of the dissipative dynamics of the single disk and those of the uniform mode of the chain of identical discs:

$$\begin{aligned} D_{\mathrm{disc}} &= \int_0^\infty V_{\mathrm{disc}}(t)\,\mathrm{d}t \\ &\equiv \int_0^\infty V_{\rho_1}(t)\,\mathrm{d}t \\ &= \frac{kT}{\gamma} \\ &\equiv D_1 \end{aligned} \tag{2.34}$$

The integral of all other normal modes of the velocity autocorrelation function are zero. Hence, the twisting diffusion coefficient for the entire set of N discs is $D_{\|} = D_1/N$.

The decay rate of the velocity autocorrelation function, $v_1(t)$, is $B_1 = \gamma/I$. This leads to a relation between diffusion and viscous drag called the Hubbard relation[37,70] in magnetic resonance literature:

$$D_1B_1 = \frac{\gamma}{I}\frac{kT}{\gamma} = \frac{kT}{I} \tag{2.35}$$

This useful relation connects the decays of the velocity position correlation functions. Notice that the decay of the velocity auto correlation is independent of the number of discs:

$$B_{\|} = B_1 = \frac{\gamma}{I} = \frac{N\gamma}{NI} \tag{2.36}$$

This is because both the friction and inertial tensor elements scale with the number of discs. Similar relations will be developed for the bending modes below.

The diffusion coefficient matrix for the entire system is the integral over the complete set of velocity correlation functions:

$$\begin{aligned} \mathbf{D}_{\|} &= \int_o^\infty \mathbf{V}(t)\,\mathrm{d}t \\ &= \mathbf{Q}\int_0^\infty \mathbf{V}_\rho(t)\,\mathrm{d}t\mathbf{Q}^\dagger \\ &= \mathbf{Q}\mathbf{E}\mathbf{Q}^\dagger\frac{kT}{\gamma} \\ &= \frac{D_1}{N}\begin{bmatrix} 1 & 1 & \cdots \\ 1 & 1 & \\ \vdots & & \ddots \end{bmatrix} \end{aligned} \tag{2.37}$$

where $\mathbf{E} \equiv \mathbf{1} - \mathbf{\Lambda}^{-1}\mathbf{\Lambda}$ contains a single nonzero element, $E_{i,j} = \delta_{j,1}\delta_{i,1}$. This result shows that each and every element of the $N \times N$ matrix for the parallel rotational diffusion tensor, $\mathbf{D}_{\|}$, has the same value and that its magnitude is $1/N$ times the coefficient for a single disk.

2.B. Bending. In our development of the bending correlation functions, we shall follow closely the definitions found in the WBR model as described by Song et al.,[5] except our model will use, as its fundamental building blocks, cylindrical discs with height, $h = 3.4$ Å and a radius on the order of $r = 12$ Å rather than the larger spheres used by Song et al. The parallels between the two models and our justification for this modification can be found elsewhere.[32,71]

The weakly bending rod consists of N cylinders. $N - 1$ bond vectors, $\mathbf{h}_i$ of length h, between the N cylindrical subunits of this rod point from the center of the ith to the center of the $(i + 1)$th disk. A bending spring, with elastic constant, κ, serves to resist deformations of the bond vectors away from the z axis of the rod. The z axis is an end-to-end vector that passes through the center-of-mass of the string of discs. In order to separate bending from twisting, the rod is assumed to experience no twisting torques since twisting motions have already been accounted for in the twisting theory. In this local molecular frame, instantaneous x and y axes are assigned to the rod, and, having removed any twisting deformations, the projection of the bond vectors onto the local x and y coordinates can be used as a measure of bending motions. Although the potential energy of deformation is a function of the polar angle between successive bond vectors, the Langevin equations of motion are more readily solved in terms of the x−y projections. If η_i is the angle between the projection of the ith bond vector in the yz plane and the z axis, then the potential energy is given by

$$U = \frac{\kappa}{2}\eta^t\mathbf{A}\eta \tag{2.38}$$

where

$$\mathbf{A} = \begin{pmatrix} -1 & 1 & 0 \\ 1 & -2 & 1 \\ 0 & 1 & \ddots \end{pmatrix} \tag{2.39}$$

is now an $(N - 1) \times (N - 1)$ matrix.

Assuming the rod deforms only weakly, the following linearization connects translational motions in the $\hat{y}$ direction of the local Cartesian coordinate system with bending deformations η_i:

$$\sin(\eta_i) = \frac{(y_{i+1} - y_i)}{h} \approx \eta_i \tag{2.40}$$

An equivalent expression is used for displacement in the $\hat{x}$ direction, wherein the angle between the projection of the ith

bond vector in the xz plane and the z axis is ξ_i. By performing this change of variables, the dynamics of bending are describable by translational Langevin equations whose solution can be found. Furthermore, these equations can be modified so as to closely resemble the twisting Langevin equations, so that the solutions we have already found for correlations in that problem are directly applicable here.

Note that there are only $N - 1$ such angles between the N subunits unlike the twisting problem where every cylinder possesses a twist angle. In matrix form, the angle $\boldsymbol{\eta}$ and displacements $\mathbf{y}$ are related by

$$\eta = \frac{1}{h}\delta\mathbf{y} \tag{2.41}$$

where

$$\delta = \begin{pmatrix} -1 & 1 & 0 & 0 \\ 0 & -1 & 1 & 0 \\ 0 & 0 & \ddots & \ddots \end{pmatrix} \tag{2.42}$$

is an $(N - 1) \times N$ difference matrix.

From the energy of the system and the principles of equilibrium statistical mechanics, we find that the same-time auto- and cross-correlation functions for bending are[21,52]

$$\langle \eta(t)\eta^{\dagger}(t)\rangle = \frac{kT}{\kappa}\mathbf{A}^{-1} \tag{2.43}$$

As is true for twisting, $\mathbf{A}^{-1}$ is the pseudo-inverse because one eigenvalue of $\mathbf{A}$ is zero. Because EPR measurements can measure only properties that depend on the autocorrelation of the angular velocity, the lowest eigenvalue and eigenvector that correspond to uniform translation are omitted from the analysis. In doing so, we are free to select subunits of identical geometry for both the twisting and the bending problems. This simplification is not possible if the theory must correctly account for rigid-body translational diffusion, an objective that lies behind the choice of larger spheres in the original WBR model.

The transformation in eq 2.41 allows us to write a translational Langevin equation of motion that correctly includes hydrodynamic interactions between subunits:

$$m\ddot{\mathbf{y}} + \gamma\dot{\mathbf{y}} + \frac{\kappa}{h^2}\mathbf{HDy} = \mathbf{F} \tag{2.44}$$

where m is the mass of each cylindrical disk, γ is the translation friction factor, $\mathbf{F}$ is the matrix of random forces, and $\mathbf{H}$ is the hydrodynamic interaction tensor. $\mathbf{H}$ is, in turn, a sum of the identity matrix and the Rotne−Prager tensor:

$$\mathbf{H} = \mathbf{1} + \mathbf{T} \tag{2.45}$$

$\mathbf{T}$ is a real, symmetric Toeplitz matrix that is accurate for the equilibrium position of the rod and hence to all thermally accessible states of deformation in the WBR limit.[5] Finally, we set the matrix $\mathbf{D}$ equal to the product of the $\mathbf{A}$ and difference matrices:

$$\mathbf{D} = \delta^{\dagger}\mathbf{A}\delta \tag{2.46}$$

We can now reverse the transformation from η to y and write the equation of motion (2.44) in terms of the angular coordinates rather than the displacement coordinates:

$$I^{\mathrm{B}}\ddot{\eta} + \gamma^{\mathrm{B}}\dot{\eta} + \kappa\underset{\sim}{\mathbf{H}}\mathbf{A}\eta = \mathbf{R} \tag{2.47}$$

where

$$\underset{\sim}{\mathbf{H}} = \delta\mathbf{H}\delta^{\dagger} \tag{2.48}$$

and $\mathbf{R} = h\boldsymbol{\delta}F$, $I^{\mathrm{B}} = h^2m$, and $\gamma^{\mathrm{B}} = h^2\gamma$. This series of transformations from angular to Cartesian and back to angular coordinates is performed to (1) correctly include hydrodynamic interactions and (2) solve directly for the angular correlation functions. The reduced hydrodynamic matrix, $\underset{\sim}{\mathbf{H}}$, shares the same properties as the hydrodynamic matrix, $\mathbf{H}$, in that it is real and symmetric, can be inverted, and has all positive eigenvalues. $\mathbf{H}$ and $\underset{\sim}{\mathbf{H}}$ contain none of the adjustable parameters and are constant matrices that depend only on the number of subunits in the WBR. We can transform this problem to one that is identical to the twisting problem by symmetrizing eq 2.47. Using the property that $(\underset{\sim}{\mathbf{H}}^{1/2})^{\dagger} = \underset{\sim}{\mathbf{H}}^{1/2}$ we write a symmetric, but wholly equivalent, equation of motion:

$$I^{\mathrm{B}}\ddot{\zeta} + \gamma^{\mathrm{B}}\dot{\zeta} + \kappa\underset{\sim}{\mathbf{A}}\zeta = \underset{\sim}{\mathbf{H}}^{-1/2}\mathbf{R} \tag{2.49}$$

where $\zeta \equiv \underset{\sim}{\mathbf{H}}^{-1/2}\boldsymbol{\eta}$, and $\underset{\sim}{\mathbf{A}} = \underset{\sim}{\mathbf{H}}^{1/2}\mathbf{A}\underset{\sim}{\mathbf{H}}^{1/2}$. The definition for $\underset{\sim}{\mathbf{A}}$, $\underset{\sim}{\mathbf{A}} = \underset{\sim}{\mathbf{H}}^{1/2}\mathbf{A}\underset{\sim}{\mathbf{H}}^{1/2}$, seems to suggest that

$$\underset{\sim}{\mathbf{A}}^{-1} = \left(\underset{\sim}{\mathbf{H}}^{1/2}\mathbf{A}\underset{\sim}{\mathbf{H}}^{1/2}\right)^{-1} \overset{?}{=} \underset{\sim}{\mathbf{H}}^{-1/2}\mathbf{A}^{-1}\underset{\sim}{\mathbf{H}}^{-1/2} \tag{2.50}$$

or

$$\mathbf{A}^{-1} \overset{?}{=} \underset{\sim}{\mathbf{H}}^{1/2}\underset{\sim}{\mathbf{A}}^{-1}\underset{\sim}{\mathbf{H}}^{1/2} \tag{2.51}$$

However, because $\mathbf{A}$ and hence $\underset{\sim}{\mathbf{A}}$ are singular matrices and because their inverses are only pseudo-inverses ($\mathbf{A}\cdot\mathbf{A}^{-1} \neq \mathbf{1}$), the second parts of eq 2.50 and eq 2.51 are not identities. The two sides of these equations differ in practice by a few percent.

From these definitions, it follows that the bending displacement, $\mathbf{C}^{\mathrm{B}}(t)$, and velocity, $\mathbf{V}^{\mathrm{B}}(t)$, correlation functions are expressible in terms of ζ:

$$\mathbf{C}^{\mathrm{B}}(t) = \langle \eta(t)\eta^{\dagger}(0)\rangle$$

$$= \underset{\sim}{\mathbf{H}}^{1/2}\langle \zeta(t)\zeta^{\dagger}(0)\rangle\underset{\sim}{\mathbf{H}}^{1/2} \tag{2.52}$$

and

$$\mathbf{V}^{\mathrm{B}}(t) = \langle \dot{\eta}(t)\dot{\eta}^{\dagger}(0)\rangle$$

$$= \underset{\sim}{\mathbf{H}}^{1/2}\langle \dot{\zeta}(t)\dot{\zeta}^{\dagger}(0)\rangle\underset{\sim}{\mathbf{H}}^{1/2} \tag{2.53}$$

This problem now is indeed identical in form to the twist problem. $\underset{\sim}{\mathbf{A}}$ can be diagonalized by an orthogonal transformation, $\underset{\sim}{\mathbf{Q}}^{\mathrm{B}}$:

$$\underset{\sim}{\mathbf{Q}}^{\mathrm{B}\dagger}\underset{\sim}{\mathbf{A}}\underset{\sim}{\mathbf{Q}}^{\mathrm{B}} = \Lambda^{\mathrm{B}} \tag{2.54}$$

so eq 2.49 is transformed into a normal mode problem that exactly parallels the twisting motion differential equation:

$$I^{\mathrm{B}}\ddot{\rho} + \gamma^{\mathrm{B}}\dot{\rho} + \kappa\Lambda^{\mathrm{B}}\rho = \mathbf{Q}^{\mathrm{B}\dagger}\underset{\sim}{\mathbf{H}}^{-1/2}\mathbf{R} \tag{2.55}$$

The solution to eq 2.55 is found by following the procedure used in the twisting problem. The resulting formula for normal mode bending angular correlation functions is[21,52]

$$\mathbf{C}_{\rho}^{\mathrm{B}}(t)=\frac{kT}{2\kappa}(\Lambda^{\mathrm{B}})^{-1}[(\mathbf{1}-(\mathbf{S}^{\mathrm{B}})^{-1})\,\mathrm{e}^{-\mathbf{r}_{+}^{\mathrm{B}}t}+(\mathbf{1}+(\mathbf{S}^{\mathrm{B}})^{-1})\,\mathrm{e}^{-\mathbf{r}_{-}^{\mathrm{B}}t}] \tag{2.56}$$

and, for the bending motions themselves:

$$\mathbf{C}^{\mathrm{B}}(t)=(\underset{\sim}{\mathbf{H}}^{1/2}\underset{\sim}{\mathbf{Q}}^{\mathrm{B}})\mathbf{C}_{\rho}^{\mathrm{B}}(t)(\underset{\sim}{\mathbf{H}}^{1/2}\underset{\sim}{\mathbf{Q}}^{\mathrm{B}})^{\dagger} \tag{2.57}$$

Again, the understanding is that the singular eigenvalue of the $\mathbf{\Lambda}^{\mathrm{B}}$ matrix is removed from the inverse and the uniform mode is treated separately. At time zero, the term in the brace of eq 2.56) reduces to a constant, and the time independent correlation functions[52] then are:

$$\mathbf{C}^{\mathrm{B}}(0)=\frac{kT}{\kappa}(\underset{\sim}{\mathbf{H}}^{1/2}\underset{\sim}{\mathbf{Q}}^{\mathrm{B}})(\Lambda^{\mathrm{B}})^{-1}(\underset{\sim}{\mathbf{H}}^{1/2}\underset{\sim}{\mathbf{Q}}^{\mathrm{B}})^{\dagger}=\frac{kT}{\kappa}\underset{\sim}{\mathbf{H}}^{1/2}\underset{\sim}{\mathbf{A}}^{-1}\underset{\sim}{\mathbf{H}}^{1/2} \tag{2.58}$$

From the equilibrium condition imposed by the laws of statistical mechanics, the result for the initial correlation functions must satisfy

$$\mathbf{C}^{\mathrm{B}}(0)=\frac{kT}{\kappa}\mathbf{A}^{-1} \tag{2.59}$$

$\mathbf{C}^{\mathrm{B}}(0)$ is used as a boundary condition to adjust the initial amplitudes of the bending displacement correlation functions:

$$\mathbf{C}^{\mathrm{B}}(t)=\frac{kT}{2\kappa}\mathbf{A}^{-1}(\underset{\sim}{\mathbf{H}}^{-\frac{1}{2}}\underset{\sim}{\mathbf{Q}}^{\mathrm{B}})[(\mathbf{1}-(\mathbf{S}^{\mathrm{B}})^{-1})\,\mathrm{e}^{-\mathbf{r}_{+}^{\mathrm{B}}t}+(\mathbf{1}+(\mathbf{S}^{\mathrm{B}})^{-1})\,\mathrm{e}^{-\mathbf{r}_{-}^{\mathrm{B}}t}](\underset{\sim}{\mathbf{H}}^{\frac{1}{2}}\underset{\sim}{\mathbf{Q}}^{\mathrm{B}})^{\dagger} \tag{2.60}$$

where

$$\mathbf{A}^{-1}=(\underset{\sim}{\mathbf{H}}^{\frac{1}{2}}\underset{\sim}{\mathbf{Q}}^{\mathrm{B}})(\Lambda^{\mathrm{B}})^{-1}(\underset{\sim}{\mathbf{H}}^{\frac{1}{2}}\underset{\sim}{\mathbf{Q}}^{\mathrm{B}})^{\dagger} \tag{2.61}$$

This replacement now guarantees that the time evolution will be consistent with the differential equation of motion, and that the time zero values will be consistent with that from the equilibrium statistical mechanics.[21]

We can employ the relation derived in eq 2.25 to immediately write down expressions for the velocity correlation functions:

$$\mathbf{V}_{\rho}^{\mathrm{bending}}(t)=\langle\dot{\rho}(t)\dot{\rho}^{\dagger}(0)\rangle$$

$$=\frac{kT}{I^{\mathrm{B}}}\frac{(\mathbf{S}^{\mathrm{B}})^{-1}}{2}\{(1+\mathbf{S}^{\mathrm{B}})\,\mathrm{e}^{-\mathbf{r}_{+}^{\mathrm{B}}t}-(1-\mathbf{S}^{\mathrm{B}})\,\mathrm{e}^{-\mathbf{r}_{-}^{\mathrm{B}}t}\} \tag{2.62}$$

where

$$r_{\pm}^{\mathrm{B}}=\frac{\gamma^{\mathrm{B}}}{I^{\mathrm{B}}}\frac{\{1\pm\mathbf{S}^{\mathrm{B}}\}}{2} \tag{2.63}$$

and

$$\mathbf{S}^{\mathrm{B}}=\sqrt{1-4\Lambda^{\mathrm{B}}\frac{(\kappa/\gamma^{\mathrm{B}})}{(\gamma^{\mathrm{B}}/I^{\mathrm{B}})}} \tag{2.64}$$

in complete analogy with the twisting functions.

From eq 2.54,

$$\Lambda^{\mathrm{B}}=\underset{\sim}{\mathbf{Q}}^{\mathrm{B}\dagger}\underset{\sim}{\mathbf{A}}\underset{\sim}{\mathbf{Q}}^{\mathrm{B}}=\underset{\sim}{\mathbf{Q}}^{\mathrm{B}\dagger}\underset{\sim}{\mathbf{H}}^{1/2}\mathbf{A}\underset{\sim}{\mathbf{H}}^{1/2}\underset{\sim}{\mathbf{Q}}^{\mathrm{B}}=(\underset{\sim}{\mathbf{H}}^{1/2}\underset{\sim}{\mathbf{Q}}^{\mathrm{B}})^{\dagger}\mathbf{A}(\underset{\sim}{\mathbf{H}}^{1/2}\underset{\sim}{\mathbf{Q}}^{\mathrm{B}}) \tag{2.65}$$

$(\underset{\sim}{\mathbf{H}}^{1/2}\underset{\sim}{\mathbf{Q}}^{\mathrm{B}})$ is a matrix that diagonalizes $\mathbf{A}$ to generate the eigenvalues of $\underset{\sim}{\mathbf{A}}$. $(\underset{\sim}{\mathbf{H}}^{1/2}\underset{\sim}{\mathbf{Q}}^{\mathrm{B}})$ is not unitary, but the unitary transformation of $\underset{\sim}{\mathbf{A}}$ by $\underset{\sim}{\mathbf{Q}}^{\mathrm{B}}$ gives the proper eigenvalues. These values are not the same as the those of $\mathbf{A}$. Note also that, even in the absence of the Rotne−Prager tensor, the eigenvalues of the bending would still resemble the square of the eigenvalues of the twisting problem, since the matrix $\underset{\sim}{\mathbf{A}}$ is analogous to a fourth order difference expression, whereas $\mathbf{A}$ by itself is analogous to a second order difference expression.

An examination of the velocity autocorrelation function shows that, at time zero,

$$\mathbf{V}^{\mathrm{B}}(0)=\frac{kT}{I^{\mathrm{B}}}\underset{\sim}{\mathbf{H}} \tag{2.66}$$

Unlike the case for twisting motions, the single disk diffusion coefficient, $D_{\mathrm{disk}}^{\mathrm{B}}=kT/\gamma^{\mathrm{B}}$, is not identical to that of the uniform mode, D_{1}^{B}, because of the hydrodynamic interactions involved. Instead, the magnitude of the uniform mode diffusion is reduced in proportion to the number of beads squared. The diffusion matrix for the entire system is the integral over the velocity correlation matrix:

$$\mathbf{D}_{\perp}^{\mathrm{B}}=\int_{0}^{\infty}\mathbf{V}^{\mathrm{B}}(t)\,\mathrm{d}t=(\underset{\sim}{\mathbf{H}}^{\frac{1}{2}}\underset{\sim}{\mathbf{Q}}^{\mathrm{B}})\Big[\int_{0}^{\infty}\mathbf{V}_{\rho}^{\mathrm{B}}(t)\,\mathrm{d}t\Big](\underset{\sim}{\mathbf{H}}^{\frac{1}{2}}\underset{\sim}{\mathbf{Q}}^{\mathrm{B}})^{\dagger}=\frac{kT}{\gamma^{\mathrm{B}}}(\underset{\sim}{\mathbf{H}}^{\frac{1}{2}}\underset{\sim}{\mathbf{Q}}^{\mathrm{B}})\mathbf{E}^{\mathrm{B}}(\underset{\sim}{\mathbf{H}}^{\frac{1}{2}}\underset{\sim}{\mathbf{Q}}^{\mathrm{B}})^{\dagger} \tag{2.67}$$

Alternatively, one can write

$$\mathbf{D}_{\perp}^{\mathrm{B}}=D_{1}^{\mathrm{B}}\underset{\sim}{\mathbf{H}}^{\frac{1}{2}}(\mathbf{1}-\underset{\sim}{\mathbf{A}}^{-1}\underset{\sim}{\mathbf{A}})\underset{\sim}{\mathbf{H}}^{\frac{1}{2}} \tag{2.68}$$

Only the uniform mode contributes to the perpendicular rotational diffusion; therefore, every element of $\mathbf{D}_{\perp}^{\mathrm{B}}$ is the same as every other element. $\mathbf{E}^{\mathrm{B}}$ contains a single nonzero element; that is, $E^{\mathrm{B}}{}_{i,j}=\delta_{j,1}\delta_{i,1}$ and $\mathbf{E}^{\mathrm{B}}=\mathbf{1}-(\mathbf{\Lambda}^{\mathrm{B}})^{-1}\mathbf{\Lambda}^{\mathrm{B}}$. As such, the matrix, $\mathbf{D}_{\perp}^{\mathrm{B}}$, can be written in terms of the pseudo-inverse matrix, which does not contain the uniform mode. The subtraction of $(\mathbf{\Lambda}^{\mathrm{B}})^{-1}\mathbf{\Lambda}^{\mathrm{B}}$ from the identity removes the internal modes contributions and leaves only the uniform mode to contribute to $\mathbf{D}_{\perp}^{\mathrm{B}}$. The numerical value of the diffusion coefficients has been developed by Song et al.[52] The relationship between the entries in $\mathbf{D}_{\perp}^{\mathrm{B}}$ is not so simply related to D_{1}^{B} as is true with twisting, but the magnitude of ratio of $\mathbf{D}_{\perp}^{\mathrm{B}}$ over D_{1}^{B} is $\sim 1/N^{2}$.

The Fourier transforms of the velocity correlation functions that are required for the calculation of $R_{1\mathrm{e}}$ are easily derived from the above expressions. As a demonstration, we consider a general Fourier−Laplace transform (FLT) of the bending velocity correlation matrix. We indicate the FLT variable by a tilde over the quantity transformed.

$$\widetilde{\mathbf{V}}^{\mathrm{B}}(w)=(\underset{\sim}{\mathbf{H}}^{\frac{1}{2}}\underset{\sim}{\mathbf{Q}}^{\mathrm{B}})\Big(\int_{0}^{\infty}\mathrm{e}^{-wt}\mathbf{V}_{\rho}^{\mathrm{B}}(t)\,\mathrm{d}t\Big)(\underset{\sim}{\mathbf{H}}^{\frac{1}{2}}\underset{\sim}{\mathbf{Q}}^{\mathrm{B}})^{\dagger}$$

$$=\frac{kT}{I^{\mathrm{B}}}(\underset{\sim}{\mathbf{H}}^{\frac{1}{2}}\underset{\sim}{\mathbf{Q}}^{\mathrm{B}})\frac{(\mathbf{S}^{\mathrm{B}})^{-1}}{2}\Big(\int_{t=0}^{\infty}\mathrm{e}^{-wt}[(\mathbf{1}+\mathbf{S}^{\mathrm{B}})\,\mathrm{e}^{-\mathbf{r}^{\mathrm{B}}t}-(\mathbf{1}-\mathbf{S}^{\mathrm{B}})\,\mathrm{e}^{-\mathbf{r}^{\mathrm{B}}t}]\mathrm{d}t\Big)(\underset{\sim}{\mathbf{H}}^{\frac{1}{2}}\underset{\sim}{\mathbf{Q}}^{\mathrm{B}})^{\dagger}$$

$$=\frac{kT}{I^{\mathrm{B}}}(\underset{\sim}{\mathbf{H}}^{\frac{1}{2}}\underset{\sim}{\mathbf{Q}}^{\mathrm{B}})\frac{(\mathbf{S}^{\mathrm{B}})^{-1}}{2}\Big[(\mathbf{1}+\mathbf{S}^{\mathrm{B}})\frac{1}{w\mathbf{1}+\mathbf{r}^{\mathrm{B}}}-(\mathbf{1}-\mathbf{S}^{\mathrm{B}})\frac{1}{w\mathbf{1}+\mathbf{r}^{\mathrm{B}}}\Big](\underset{\sim}{\mathbf{H}}^{\frac{1}{2}}\underset{\sim}{\mathbf{Q}}^{\mathrm{B}})^{\dagger} \tag{2.69}$$

where the transform variable, w is

$$w = i\omega + r_0 \qquad r_0 \geq 0 \tag{2.70}$$

Equation 2.69 is the most general form of the FLT that we will need for the velocity autocorrelation functions. It subsumes the uniform mode of motion and contains only the bending force constant, κ, as an adjustable parameter. (The number of subunit discs is known a priori and the disk friction factors are calculated from well-known expressions for cylinders.[72,73]) In the limit as the moment of inertia goes to zero, one can obtain a simplified expression for $\tilde{\mathbf{V}}^{\mathrm{B}}(w)$:

$$\lim_{I\to 0}\widetilde{\mathbf{V}}^{\mathrm{B}}(w) = \frac{kT}{\gamma^{\mathrm{B}}}\underset{\sim}{\mathbf{H}}^{\frac{1}{2}}\mathbf{Q}^{\mathrm{B}}\left[\mathbf{1} - \frac{\kappa}{\gamma^{\mathrm{B}}}\Lambda^{\mathrm{B}}\left(w\mathbf{1} + \frac{\kappa}{\gamma^{\mathrm{B}}}\underset{\sim}{\mathbf{A}}\right)^{-1}\right]\mathbf{Q}^{\mathrm{B}\dagger}\underset{\sim}{\mathbf{H}}^{\frac{1}{2}}$$

$$= \frac{kT}{\gamma^{\mathrm{B}}}\underset{\sim}{\mathbf{H}}^{\frac{1}{2}}\left[\mathbf{1} - \frac{\kappa}{\gamma^{\mathrm{B}}}\underset{\sim}{\mathbf{A}}\left(w\mathbf{1} + \frac{\kappa}{\gamma^{\mathrm{B}}}\underset{\sim}{\mathbf{A}}\right)^{-1}\right]\underset{\sim}{\mathbf{H}}^{\frac{1}{2}} \tag{2.71}$$

The FLT of the angular velocity correlation functions for the twisting modes of motion is given by

$$\widetilde{\mathbf{V}}(w) = \mathbf{Q}\left(\int_0^\infty \mathrm{e}^{-wt}\mathbf{V}_\rho(t)\,\mathrm{d}t\right)\mathbf{Q}^\dagger$$

$$= \mathbf{Q}\frac{(\mathbf{S})^{-1}}{2}\left[(\mathbf{1}+\mathbf{S})\frac{1}{w\mathbf{1}+\mathbf{r}_+} - (\mathbf{1}-\mathbf{S})\frac{1}{w\mathbf{1}+\mathbf{r}_-}\right]\mathbf{Q}^\dagger \tag{2.72}$$

Taking the same limit as the moment of inertia goes to zero gives

$$\lim_{I\to 0}\tilde{\mathbf{V}}(w) = \frac{kT}{\gamma}\left[\mathbf{1} - \frac{\alpha}{\gamma}\mathbf{A}\left(w\mathbf{1} + \frac{\alpha}{\gamma}\mathbf{A}\right)^{-1}\right] \tag{2.73}$$

These FLT forms will be needed for the spectral density functions that will be introduced later in our work. In particular, eq 2.71 and eq 2.73 are needed to describe the spin rotation mechanism.

3. Relationship of the Lipari−Szabo (L−S) Formalism to the Weakly Bending Rod Model. As has been shown by Schurr, correlation functions between WRM elements arise naturally in the context of magnetic resonance relaxation theory.[8] These WRM correlations are, in turn, related to the correlation functions for the angular displacements. Specifically:

$$G_{p,p'}(t) = \delta_{q,q'}\langle D^l_{p',q'}(\Omega(t))D^l_{p,q}(\Omega(0))\rangle \tag{3.1}$$

where

$$\langle D^l_{p',q}{}^*(\Omega(t))D^l_{p,q}(\Omega(0))\rangle = \delta_{p,p'}\frac{1}{2l+1}\times$$

$$\exp\left[-((l(l+1)) - p^2)\frac{\langle\Delta x^2(t)\rangle}{2}\right]\exp\left[-p^2\frac{\langle\Delta z^2(t)\rangle}{2}\right] \tag{3.2}$$

and the displacements along x and z refer to the bth disk and are the autocorrelations of that disk. The Cartesian displacements can be written in terms of angular difference correlation functions. For bending, the difference correlation function in angles is

$$\frac{1}{2}\langle\Delta x_b^2(t)\rangle = D_\perp t + \frac{1}{2}\langle[\eta_b(t) - \eta_b(0)]^2\rangle \tag{3.3}$$

and for twisting, it is

$$\frac{1}{2}\langle\Delta z_b^2(t)\rangle = D_\parallel t + \frac{1}{2}\langle[\phi_b(t) - \phi_b(0)]^2\rangle \tag{3.4}$$

These angular correlation functions are separated into the uniform modes, characterized by the overall diffusion coefficients $D_\perp$ and $D_\parallel$, defined above in eq 2.68 and eq 2.37, and the internal motions of bending and twisting, defined in eq 2.60 and eq 2.18. Now consider the correlation function for the bth disk. The relationship between the difference correlation function in eq 3.4 and the correlation functions derived above for the internal twisting motions of the WBR is

$$\frac{1}{2}\langle[\phi_b(t) - \phi_b(0)]^2\rangle = [\mathbf{C}(0) - \mathbf{C}(t)]_{b,b} \tag{3.5}$$

Similarly, the relationship for the internal bending motions is

$$\frac{1}{2}\langle[\eta_b(t) - \eta_b(0)]^2\rangle = [\mathbf{C}^{\mathrm{B}}(0) - \mathbf{C}^{\mathrm{B}}(t)]_{b,b} \tag{3.6}$$

Combining eqs 3.1 through 3.3 and eq 3.6, we obtain for the internal bending mode contribution to the position correlation function:

$$\exp[-((l(l+1)) - p^2)[\mathbf{C}^{\mathrm{B}}(0) - \mathbf{C}^{\mathrm{B}}(t)]_{b,b}] \tag{3.7}$$

A similar equation for twisting is given by

$$\exp[-p^2[\mathbf{C}(0) - \mathbf{C}(t)]_{b,b}] \tag{3.8}$$

Equations 3.7 and 3.8 are 1 at $t = 0$ and approach a constant at $t \to \infty$. This is because the internal modes are zero at time zero and build to the constant $(\mathbf{C}^{\mathrm{B}}(0))_{b,b}$ or $(\mathbf{C}(0))_{b,b}$ at large times. These forms guarantee that the correlation functions decrease as time t increases. Schurr and co-workers demonstrate that this property of internal modes results in an amplitude reduction factor to the correlation functions.[8,50,74] If the decay rate of the internal modes is rapid compared with the uniform modes, the primary effect of internal motion is to reduce the amplitude of the correlation functions. This reduction then carries over directly to the spectral density function, or the Fourier transform of the correlation function, and hence reduces the relaxation rate accordingly. The difficulty of developing analytic formulas for the spectral density functions is that the correlation functions in eq 3.5 and eq 3.6 are sums of exponential terms in the WBR model. Then, eq 3.7 becomes the exponential of exponentials. Calculation of the spectral density, eq 1.4, requires a FT of the resulting exponential of exponentials, a transform for which there is no closed analytic solution.

Lipari and Szabo (L−S) formulated a model free[47] (or a generalized model) method to account for the effects of internal motions and thereby circumvented the transform impasse. In the L−S model, any model-specific manifestations of the correlation functions in eq 3.7 or eq 3.8 are subsumed in a model-independent expression. The equivalence is expressed simply as

$$\exp[-p^2[\mathbf{C}^{\mathrm{B}}(0) - \mathbf{C}^{\mathrm{B}}(t)]_{b,b}] \triangleq \boldsymbol{S}^2 + (\mathbf{1} - \boldsymbol{S}^2)\exp[-t/\tau_I] \tag{3.9}$$

$\mathbf{S}^2$ is the square order parameter, or the amplitude reduction factor. Lipari and Szabo recognized that the equivalence was justified since at time zero both sides of eq 3.9 are one, and as $t \to \infty$, both approach a constant value.

In order for the two forms to be equal at infinite time, it is required that $\exp[-p^2[C^{\mathrm{B}}(0)]_{b,b}] = \mathbf{S}^2$. The time constant, τ_I, is an effective relaxation time associated with the internal dynamics. The L−S equation is simple and treats the internal motion as relaxing according to a single exponential. In contrast, the WBR model is anisotropic in the sense that its correlation functions depend on the integer p and in general contain both

twisting and bending processes that decay independently. Lipari and Szabo consider the possibility of including additional internal dynamics to accommodate such anisotropic motion, but these extensions introduce adjustable parameters for which no tie to a physical model exists to provide substance for their interpretation. The WBR model, on the other hand, automatically produces anisotropic decay to accommodate data with complex relaxation dynamics, and introduces only the twisting force constant, α, the bending force constant, κ, and the number of discs as its physically relevant parameters.

The disadvantage of a direct application of the WBR results to a practical analysis of EPR data is the added complexity of the functional forms and summations in the correlation functions. Our effort is to find a general function of the L−S form that can capture the effects of the correlation functions predicted by the WBR and maintain the simplicity suggested by Lipari and Szabo. To that end, we have explored equating the WBR model relaxation functions to stretched exponentials. This is motivated in part by the observations of Schurr and co-workers that in the intermediate motion regime the twisting dynamics have the appearance of being not just exponential in time[4] or $\exp[-t/\tau]$, but also decaying as the square root of time or $\exp[-(t/\tau)^{\beta}]$, where $\beta \sim 1/2$, and that bending dynamics have a similar form[8] and $\beta \sim 1/4$. The general form of the decay then is examined as a series of stretched exponentials.

Therefore, we consider fitting varied numerical decay curves from the twisting correlation functions for the internal modes as

$$\exp\left[-p^2[\mathbf{C}(0)-\mathbf{C}(t)]_{b,b}\right]=S_p^2+(1-S_p^2)\exp\left[-\left(\frac{t}{\tau_p}\right)^{\beta_p}\right] \tag{3.10}$$

where

$$S_p^2=\exp\left[-p^2[\mathbf{C}(0)]_{b,b}\right] \tag{3.11}$$

The bending decay functions are similarly compared to stretched exponentials:

$$\exp\left[-((l(l+1))-p^2)[\mathbf{C}^{\mathrm{B}}(0)-\mathbf{C}^{\mathrm{B}}(t)]_{b,b}\right]= \left(S_p^{\mathrm{B}}\right)^2+\left(1-\left(S_p^{\mathrm{B}}\right)^2\right)\exp\left[-\left(\frac{t}{\tau_p^{\mathrm{B}}}\right)^{\beta_p^{\mathrm{B}}}\right] \tag{3.12}$$

where

$$\left(S_p^{\mathrm{B}}\right)^2=\exp\left[-((l(l+1))-p^2)[\mathbf{C}^{\mathrm{B}}(0)]_{b,b}\right] \tag{3.13}$$

We now wish to find the best stretched exponential in these L−S approximations to the WBR correlation functions. In order to find these, we rearrange the expressions to isolate the stretched exponentials. For twisting, we obtain

$$\exp\left[-\left(\frac{t}{\tau_p}\right)^{\beta_p}\right]=\frac{\exp\left[-p^2[\mathbf{C}(0)-\mathbf{C}(t)]_{b,b}\right]-\exp\left[-p^2\mathbf{C}(0)_{b,b}\right]}{\mathbf{1}-\exp\left[-p^2\mathbf{C}(0)_{b,b}\right]}$$

$$=\frac{\exp[p^2\mathbf{C}(t)_{b,b}]-\mathbf{1}}{\exp[p^2\mathbf{C}(0)_{b,b}]-\mathbf{1}} \tag{3.14}$$

The right-hand side of the expression is defined by the WBR model. The left-hand side contains two parameters, β_p and τ_p, that are adjusted by a least-squares method to find the best fit to the correlation functions. Similarly, isolation of the stretched exponential in eq 3.12 gives

$$\exp\left[-\left(\frac{t}{\tau_p^B}\right)^{\beta_p^B}\right]=\frac{\exp[((l(l+1))-p^2)\mathbf{C}_B(t)_{b,b}]-\mathbf{1}}{\exp[((l(l+1))-p^2)\mathbf{C}_B(0)_{b,b}]-\mathbf{1}} \tag{3.15}$$

Rather than treat twisting and bending separately as in eqs 3.10−3.15, we opt for a more generic expression that subsumes both types of motion into a general expression for the overall correlation function in terms of stretched exponentials. We define the overall correlation function as

$$G_p(t)=G_p^0(t)G_p^{\mathrm{I}}(t) \tag{3.16}$$

where

$$G_p^0(t)=\frac{1}{2l+1}\exp\left[-[((l(l+1))-p^2)D_\perp+p^2D_{||}]t\right] \tag{3.17}$$

and

$$G_p^{\mathrm{I}}(t)=\exp\left[-((l(l+1))-p^2)\langle[\eta_b(t)-\eta_b(0)]^2\rangle\right]\exp\left[-p^2\langle[\phi_b(t)-\phi_b(0)]^2\rangle\right] \tag{3.18}$$

$G_p(t)$ is the product of the decay of the uniform modes, $G_p^0(t)$, and the internal modes, $G_p^{\mathrm{I}}(t)$. At $t=0$, the internal modes do not contribute to the correlation function because $G_p^{\mathrm{I}}(0)=1$. As $t\rightarrow\infty$ or, less stringently, when t is much greater than the decay time of the longest internal modes, $\tau_{\max}^{\mathrm{I}}$, the accumulated effect of the decay of internal modes is a constant amplitude reduction factor:

$$G_{p,p'}^{\mathrm{I}}(t\gg\tau_{\max}^{\mathrm{I}})=(S_p^{\mathrm{I}})^2$$

$$=S_p{}^2(S_p^{\mathrm{B}})^2$$

$$=\exp\left[-p^2[\mathbf{C}(0)]_{b,b}\right]\exp\left[-((l(l+1))-p^2)[\mathbf{C}^{\mathrm{B}}(0)]_{b,b}\right] \tag{3.19}$$

Following the same reasoning leading up to eq 3.10 and eq 3.12, we equate a stretched exponential version of the L−S formula to eq 3.19:

$$G_{p,p'}^{\mathrm{I}}(t)=\delta_{p,p'}\left\{(S_p^{\mathrm{I}})^2+\left(1-(S_p^{\mathrm{I}})^2\right)\exp\left[-\left(\frac{t}{\tau_p^{\mathrm{I}}}\right)^{\beta_p^{\mathrm{I}}}\right]\right\} \tag{3.20}$$

This is a single internal function that combines both twist and bend. We will demonstrate how the internal correlation times and amplitudes can be given in terms of the twisting and bending parameters through the use of this equation and the least-squares fitting of the stretched exponential to the WBR correlation functions:

$$\exp\left[-\left(\frac{t}{\tau_p^{\mathrm{I}}}\right)^{\beta_p^{\mathrm{I}}}\right]= \frac{\exp\left[((l(l+1))-p^2)[\mathbf{C}^{\mathrm{B}}(t)]_{b,b}\right]\exp\left[p^2[\mathbf{C}(t)]_{b,b}\right]-1}{\exp\left[((l(l+1))-p^2)[\mathbf{C}^{\mathrm{B}}(0)]_{b,b}\right]\exp\left[p^2[\mathbf{C}(0)]_{b,b}\right]-1} \tag{3.21}$$

Aside from the dependence on the integer index p and the stretched exponential, eq 3.20 is indistinguishable from the L−S equation, 3.9. However, the correlation functions that determine the **S** parameter, as well as the stretched exponential rates, are

determined from the WBR model. Despite the apparent introduction of variables on the right-hand side of eq 3.21, only two parameters, α and κ, are adjustable once the number and geometry of disk subunits is set and the solvent conditions determined. No ad hoc introduction of additional parameters is required to account for complex relaxation rates.

4. A. Fourier Transform of the Stretched Exponential. Analytical expressions for the FT of the exponential of exponentials are unknown; this motivated the hybridization of the L−S method with the results of the WBR model. However, there are also no known analytical expressions for the FT of stretched exponentials that appear in eq 3.20. More generally, the problem of obtaining a spectral density function for a stretched exponential provides a very general tool in magnetic resonance, since there are often situations when no specific model is a candidate for description of the modes of motion. In such cases, the use of the generic form given in eq 3.20 is the only recourse. For these reasons, we now review a method to find the spectral density function of a stretched exponential.

The solution of representing the FT of a stretched exponential (also known as the Kohlrausch−Williams−Watts (KWW) function, f_{KWW}) by series expansion in terms of a set of simple exponentials decaying at different rates has been solved by Lindsey and Patterson.[55] This expansion is given by

$$f_{KWW}(t) \equiv \exp\left[-\left(\frac{t}{\tau_w}\right)^{\beta}\right] \cong \sum_{n=1}^{N} g_n \exp\left[-\frac{t}{\tau_w} r_n\right] \tag{3.22}$$

where the time constant for each exponential is given as

$$\tau_n \equiv \frac{\tau_w}{r_n} \tag{3.23}$$

The FT of the summation is easily taken if a suitable set of expansion coefficients and rates can be found:

$$\tilde{f}_{KWW}(\omega) \equiv \int_{t=0}^{\infty} \exp[-i\omega t] \exp\left[-\left(\frac{t}{\tau_w}\right)^{\beta}\right] \mathrm{d}t \cong \sum_{n=1}^{N} g_n \frac{\tau_w}{i\omega\tau_w + r_n} \tag{3.24}$$

Because of the finiteness and discreteness of the sum, the coefficients must be renormalized to guarantee that $\sum_n g_n = 1$.

The expansion in eq 3.22 is written in terms of r_n because r_n depends only on the ratio of τ_n to the stretched exponential time, τ_w. The sete of r_n is chosen on a logarithmic scale:

$$r_n = 10^{\lambda_n} \qquad -\lambda_{max} \le \lambda_n \le \lambda_{max} \tag{3.25}$$

Satisfactory results are obtained on the longest time scales required for $N \le 101$, and for values of β in the range $0.2 \le \beta \le 0.999$. The coefficients of the expansion are

$$g_n = -\left(\frac{\Delta\lambda}{\pi}\right)\sum_{k=0}^{\infty} \frac{\Gamma(\beta k+1)}{\Gamma(k+1)} \sin(\pi\beta k)\left(\frac{-1}{r_n^{\beta}}\right)^k \tag{3.26}$$

where $\Delta\lambda$ is the (equal) spacing between the values chosen for the logarithmic set of r_n values in eq 3.25.

Equation 3.26 is a divergent power series but remains numerically bounded up to about 200 terms. In fact, convergence is reached within 150 to 180 terms, so g_n is well-defined for the expansion required in eq 3.24. The terms in eq 3.26 are summed by Horner's method to obtain sufficient numerical accuracy. Despite the precautions in Horner's method, numerical instability occurs for small values of r_n for which $\lambda_n < 2(1 - 1/\beta)$. Empirically, it is found that, for these small r_n, the coefficients may be set to zero without loss of accuracy; that is, $g_n(r_n\colon \lambda_n < 2(1 - 1/\beta)) = 0$.

A useful approximation to $\tilde{f}_{KWW}(\omega)$ is given by

$$\hat{f}(\varphi) \equiv f_{\mathrm{low}} \frac{\varphi}{1 + \frac{f_{\mathrm{low}}}{f_{\mathrm{high}}}\varphi^{1+\beta}} \cong \boldsymbol{R}\{\tau\tilde{f}_{\mathrm{KWW}}(\omega)\} \tag{3.27}$$

where

$$\varphi = \omega\tau_w \tag{3.28}$$

and

$$f_{\mathrm{high}} = \frac{\beta(3-\beta)}{2} \qquad f_{\mathrm{low}} = \left(\frac{1}{\beta}\right)^{\left\{\frac{3}{4}\left(\frac{1}{\beta}-1\right)\right\}} \tag{3.29}$$

This approximation deviates slightly only for $\varphi \sim 1$. Otherwise, $\hat{f}(\varphi)$ offers a simple, descriptive, and accurate value for the spectral density from which useful statements can be made without detailed computation. This is demonstrated in Figure 4. Note that the approximation is good everywhere except in a single order of magnitude surrounding $\varphi \sim 1$.

The effort to represent the internal functions in eq 3.18 in terms of stretched exponentials in eq 3.20 which then are expanded in terms of eq 3.22, or the approximation in eq 3.27, is worthwhile for the following reasons. The internal correlation functions are solved in quasi-analytic forms that are efficiently calculated. Moreover, the dependence on only the bending and twisting force constants is retained in the quasi-analytic forms. In fact, the transformation from internal correlation functions to a stretched exponential function requires little computational effort as it is performed with robust and well-established least-squares fit protocols, such as the Levenberg−Marquardt algorithm. The further transformation from the stretched exponential representing the correlation functions to the spectral density utilizes the well-established KWW solution developed by Patterson and Lindsey and is also performed easily. Finally, the stretched exponential approach may have many general applications to magnetic resonance that go well beyond the specific applications to the WBR model used here.

4.B. Application to the WBR Model. We group together the relaxation processes from the uniform modes and define a single time constant, τ_p^0 as

$$\frac{1}{\tau_p^0} = [((l(l+1)) - p^2)D_{\perp} + p^2 D_{\|}] \tag{3.30}$$

Then the form for the spectral density function, as the FT of the correlation function, is

$$\begin{aligned} J_{p,p'} &\equiv \delta_{p,p'}\tilde{f}_p(\omega) \\ &= \frac{1}{2l+1}\int_{t=0}^{\infty} \mathrm{e}^{-i\omega t} \exp\left[-\frac{t}{\tau_p^0}\right]\left[(S_p^{\mathrm{I}})^2 + (1-(S_p^{\mathrm{I}})^2)\sum_{n=1}^{N} g_n \exp\left[-\frac{t}{\tau_p^{\mathrm{I}}} r_n\right]\right] \mathrm{d}t \\ &= \frac{1}{2l+1}\left[(S_p^{\mathrm{I}})^2 \frac{\tau_p^0}{i\omega\tau_p^0 + 1} + (1-(S_p^{\mathrm{I}})^2)\sum_{n=1}^{N} g_n \frac{\tau_p^{\mathrm{I}}}{i\omega\tau_p^{\mathrm{I}} + \frac{\tau_p^{\mathrm{I}}}{\tau_p^0} + r_n}\right] \end{aligned} \tag{3.31}$$

Equation 3.31 is the result for the spectral density function generated by replacing the internal relaxation function with a

stretched exponential form in the L−S formalism.[48,49] The parameters of the stretched exponential are determined from the WBR rod model.[8,74]

An aspect of the WBR model that we have omitted is the inclusion of an initial amplitude reduction factor which has no time dependence and parametrizes all unknown short-time processes leading to decorrelation.[8,52,74] Inclusion of this initial factor is avoided since, in magnetic resonance theory, it can be absorbed into the coupling tensors in the Hamiltonian.

5. Spectral Density Function for R_{1e}^{SR}. The one relaxation mechanism that is not well-developed in the literature is that for the spin rotation mechanism. As commented above, this involves knowing the correlation functions for the angular velocities, which are now incorporated into the overall expression for the spectral density functions from the spin rotation mechanism.

With the aid of equations developed in sections 1−4, we can write out the spectral density function $J^{SRm,m'}_{p,p'}(\omega)$ for the spin rotation mechanism:

$$J^{SRm,m'}_{p,p'}(\omega_e) = \int_{t=0}^{\infty} e^{-i\omega_e t} G^{SRm,m'}_{p,p'}(t)\, dt \tag{5.1}$$

where

$$G^{SRm,m'}_{p,p'}(\tau) = \delta_{n,n'}\langle D^{1*}(\Omega_{L-D}(0))_{p,n} D^1(\Omega_{L-D}(\tau))_{p',n'}\rangle \times \langle(\omega_I(0)\omega_I^{\dagger}(\tau))_{m,m'}\rangle \tag{5.2}$$

as introduced previously in eq 1.17 and included again here for convenient reference. For $l = 1$, we have by eq 3.30

$$\frac{1}{\tau_p^0} = [(2-p^2)D_{\perp} + p^2 D_{||}] \tag{5.3}$$

and, using the L−S−WBR formalism summarized by eq 3.31,

$$\langle D^{1*}(\Omega_{L-D}(0))_{p,n} D^1(\Omega_{L-D}(\tau))_{p',n'}\rangle = \frac{\delta_{p,p'}}{3}\exp\left[-\frac{t}{\tau_p^0}\right]\left[(S_p^I)^2 + \left(1-(S_p^I)^2\right)\sum_{n=1}^{N} g_n \exp\left[-\left(\frac{t}{\tau_p^I}\right)r_n\right]\right] \tag{5.4}$$

For the velocity correlations appearing in eq 5.2, we write

$$\langle[\omega_I(0)\omega_I^{\dagger}(\tau)]_{m,m'}\rangle_{b,b} = \begin{cases} \delta_{m,m'}[\mathbf{V}(t)]_{b,b} & m = z \\ \delta_{m,m'}[\mathbf{V}^B(t)]_{b,b} & m = x, y \end{cases} \tag{5.5}$$

The spectral density for the twisting velocity correlation functions is

$$J^{z,z}_{p,p'}(\omega) = \frac{\delta_{p,p'}}{3}\int_{t=0}^{\infty} e^{-i\omega t} e^{-t/\tau_p^0}\left[(S_p^I)^2 + \left(1-(S_p^I)^2\right)\sum_{n=1}^{N} g_n e^{-(t/\tau_p^I)r_n}\right][\mathbf{V}(t)]_{b,b'}\, dt$$

$$= \frac{\delta_{p,p'}}{3}\left[(S_p^I)^2[\widetilde{\mathbf{V}}(w)]_{b,b} + \left(1-(S_p^I)^2\right)\sum_{n=1}^{N} g_n[\widetilde{\mathbf{V}}(w_n)]_{b,b}\right] \tag{5.6}$$

where

$$w = i\omega + \frac{1}{\tau_p^0} \tag{5.7}$$

and

$$w_n = i\omega + \frac{1}{\tau_p^0} + \frac{r_n}{\tau_p^I} \tag{5.8}$$

The spectral density for the bending motions is

$$J^{x,x}_{p,p'}(\omega) = J^{y,y}_{p,p'}(\omega) = \frac{\delta_{p,p'}}{3}\left[(S_p^I)^2[\widetilde{\mathbf{V}}^B(w)]_{b,b} + \left(1-(S_p^I)^2\right)\sum_{n=1}^{N} g_n[\widetilde{\mathbf{V}}^B(w_n)]_{b,b}\right] \tag{5.9}$$

The FLT for the twisting and bending correlation functions are defined above in eqs 2.69 and 2.72. Equations 5.6 and 5.9 are two of the main results of this work.

Materials and Methods

1. Experimental Procedures for Spin−lattice Relaxation Measurements on DNA. In the spin−lattice relaxation studies presented in this work, we use a novel spin probe that is rigidly locked into the helical structure. It is a cytosine-mimic, Ç, that is synthesized and incorporated into a phosphoramidite for solid-state DNA synthesis, as described elsewhere.[10,29] DNA oligomers are synthesized on an ASM 800 DNA synthesizer from Biosset (Russia). Modified and unmodified oligonucleotides are synthesized by a trityl-off synthesis on a 1.0 μmol scale (1000 Å CPG columns) using phosphoramidites with standard base protection. All commercial phosphoramidites, columns, and solutions are purchased from ChemGenes. For spin-labeled DNA, the spin-labeled phosphoramidite is site-specifically incorporated into the oligonucleotides by manual coupling. The DNA is deprotected at 55 °C for 8 h and purified by 23% denaturing polyacrylamide gel electrophoresis (DPAGE). The oligonucleotides are visualized by UV shadowing. The bands visible in shadowing are excised from the gel, crushed, and then soaked in TEN buffer (250 mM NaCl, 10 mM Tris, 1 mM Na2EDTA, pH 7.5) for 20 h. For filtration of DNA elution solutions, 0.45 μm polyethersulfone membrane (a disposable filter device from Whatman) is used. The DNA elution solutions are desalted using Sep-Pak cartridges (Waters Corporation) according to the manufacturer's instructions. The spin-labeled sequences are then combined in a 1:1.2−1:1.5 ratio with a complementary unlabeled strand of the same length and hybridized stepwise on a thermocycler (90 °C for 2 min, 60 °C for 5 min, 50 °C for 5 min, 40 °C for 5 min, and 22 °C for 15 min) before the sample is returned to 4 °C. The final concentration of the spin-labeled DNA is between 80 and 150 μM in a 50 mM potassium 3-(*N*-morpholino) propanesulfonic acid (K-MOPS; 20 mM K^+), pH 7.0, with strand concentrations determined by absorbance at 260 nm.

In order to examine the R_{1e} results across a range of rotational correlation times, the length of the DNA is varied from 11 to 47 base-pairs, and the viscosity is adjusted between 1 and 15 cP by adding sucrose, a neutral osmolyte that does not significantly alter the internal structure of DNA.[75] For all sequences, the spin probe is incorporated at a position 7 base-pairs from the 3′-end, in reference to the spin-labeled strand. The solvent viscosity is calculated from the known sucrose concentration using well-established empirical formulas.[76] The diffusion coefficients for rigid cylinders with dimensions on the order of the DNAs used in the experiments are calculated from well-known hydrodynamic equations.[5,21,52,72,73] The spin-labeled DNA sequences are shown in Table 1. The spin labeled base is represented by Ç, in red. The original 11-mer is extended by 12 bases on the 5′-end, as indicated by blue lettering, to form 23-, 35-, and 47-mers.

TABLE 1: Sequences for DNAs Studied by pSR[a]

length [bp]	sequence
11	5′-d(CCC TÇT TGT CC)-3′
23	5′-d(**AGG TTG ATT TTG** CCC TÇT TGT CC)-3′
35	5′-d(**TGT GTA AGT TTT** AGG TTG ATT TTG CCC TÇT TGT CC)-3′
47	5′-d(**GCG GCT CCA ATG** TGT GTA AGT TTT AGG TTG ATT TTG CCC TÇT TGT CC)-3′

[a] The spin labeled base is represented by Ç. The original 11-mer is extended by 12 bases on the 5′-end to form 23-, 35-, and 47-mers. Only the spin-labeled strand of the duplex is shown; each spin-labeled sample is prepared as a duplex with its appropriate full complement. The position of the spin label is 7 with respect to the 3′-end in all cases.

Pulsed saturation recovery (pSR) spectra were acquired on a home-built EPR spectrometer with both continuous wave (CW) and pulsed saturation recovery (pSR) EPR measurement capability.[36] In order to select the appropriate magnetic field at which to perform the pSR experiment, a CW spectrum must first be collected on the pSR instrument, with resolution at 1024 points over a range of 90 Gauss during one scan at a constantly applied −12 dBm microwave power, with 1 Gauss modulation amplitude and a modulation frequency of 10 kHz. The highest spin density point is the center of the center field resonance manifold, of the three ^{14}N resonance manifolds in the CW spectrum. That highest spin density resonance position is chosen as the field position at which to apply the pump pulse for the pSR experiment. To collect data by pSR, a 200 ns pump pulse at 9.2 GHz with +20 dBm of microwave power is applied, followed by 90 ns of dead time. The response is observed with an offset of 100 kHz at −12 dBm of microwave power. The typical time resolution for a pSR spectrum in this study is 20 ns per point, for 4096 points and averaged over 4.8×10^6 scans (80% of the scans on resonance and 20% ∼100 Gauss off resonance, to allow for background subtraction). Multiple spectra were collected on multiple days, to ensure reproducibility. To determine the reliability and consistency of sample preparation, the 23-mer and 47-mer measurements were repeated with two sets of unique, independently prepared samples, and the results were statistically the same for both preparations. All samples used in the TD instrument are in a gas permeable 0.8 mm inner diameter Teflon capillary tube under a continuous stream of N_2 gas at ∼21 °C. All measured spin−lattice relaxation rates are highly reproducible. The standard deviation of each data point ranges from 0.3 to 4.5% of the mean value.

2. Computational Methods. The correlation functions and order parameters are computed according to the WBR theory and summarized in the Theory section above. We use eq 3.21 to fit the decaying correlation functions for internal motions to stretched exponentials, in a least-squares sense, using a Marquardt−Levenberg minimization algorithm. All fitting is done using programs written and executed in Matlab. One- and two-exponential fits are also tested and compared with the stretched exponential fits as shown in Table 2. The $\tau_p^I/t_{\max}$ ratio is kept reasonably constant and on average is 0.03 with a standard deviation of 0.02 for all lengths, spin label positions, and p values. The time scale, $t_{\max} \sim 30 \cdot \tau_p^I$, is chosen to be long enough to maximize fit quality but short enough that the fit is not overweighted by the nearly zero (fully decayed) part of the function. The fit to a single exponential gives about a 5- to 10-fold larger standard error than the fit to a stretched exponential. Agreement of the single exponential is good only at the early time decay and misses the middle of the autocorrelation decay. Errors on Figures 4−7, which show the results of fitting to the stretched exponentials, are within the size of the symbols. The fits are repeatable, independent of the choice of beginning estimates for the functional parameters. For all displayed figures, α/kT is kept equal to 100, as that is a reasonable approximation for α/kT for 10−200 bp DNAs under these experimental conditions.[3,4,7,8,21,77] In this work, we intend to examine the effect of changes to parameters other than α/kT.

TABLE 2: Fit of Exponential Functions to WBR Model[a]

length [bp]	κ/kT	p	τ_p^I [ns]	β_p^I
23	150	0	0.03706 ± 0.00037	0.5501 ± 0.0042
23	150	0	0.04837 ± 0.0014	1
23	150	1	0.05052 ± 0.00035	0.5547 ± 0.0029
23	150	1	0.06487 ± 0.0018	1
23	150	2	0.09311 ± 0.00052	0.6285 ± 0.0032
23	150	2	0.1113 ± 0.0025	1
23	350	0	0.01738 ± 0.00013	0.5816 ± 0.0034
23	350	0	0.02236 ± 0.00049	1
23	350	1	0.04173 ± 0.00021	0.5025 ± 0.0017
23	350	1	0.05551 ± 0.0019	1
23	350	2	0.09984 ± 0.00061	0.6348 ± 0.0035
23	350	2	0.1189 ± 0.0027	1
201	150	0	32.18 ± 0.62	0.4808 ± 0.0058
201	150	0	46.55 ± 1.8	1
201	150	1	18.75 ± 0.36	0.424 ± 0.0042
201	150	1	27.98 ± 1.3	1
201	150	2	5.081 ± 0.012	0.3936 ± 0.0042
201	150	2	9.26 ± 0.32	1
201	350	0	18.16 ± 0.32	0.5184 ± 0.0063
201	350	0	25.12 ± 0.87	1
201	350	1	10.27 ± 0.074	0.4828 ± 0.0022
201	350	1	14.13 ± 0.51	1
201	350	2	5.726 ± 0.019	0.5575 ± 0.0014
201	350	2	7.329 ± 0.19	1

[a] Included are results of fitting autocorrelation functions to either a single exponential (where $\beta = 1$) or to a stretched exponential, at 21°C, with α/kT kept equal to 100. The standard error for each parameter is shown in the column after its value.

We test a fit of the correlation functions to the sum of two standard exponentials as well as to the sum of two stretched exponentials (data not shown) and find an insignificant improvement in the fit of the data. Moreover, fitting to two stretched exponentials with separate decay rates and β_p^I exponential values is overparameterized for reliable convergence. All comparative tests are done for either a middle-labeled 23-mer or a middle-labeled 201-mer.

Results

1. Experimental Data Motivating Theoretical Development. We have recently carried out pSR-EPR experiments to measure for the first time the R_{1e} of a spin probe in a series of duplex DNAs. The DNA is duplexes of length 11, 23, 35, and 47 base-pairs. Figure 1 illustrates the spin probe, Ç, base-paired to a natural guanine.[29] Figure 2a shows the R_{1e} values as a function of the geometrically averaged rotational correlation time, $\langle \tau_{perp}^2 \tau_{para} \rangle^{1/3}$ for the overall rotational motion of the duplex DNA.[72,73] The solid line shows the predicted R_{1e} values for a range of rotational correlation times, based on the relaxation

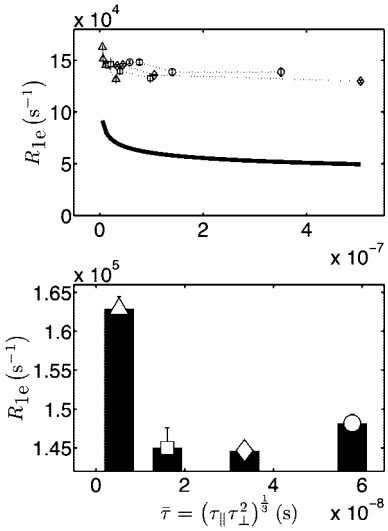

Figure 2. Experimental R_{1e} data for 11- to 47-mer duplex DNAs in varying viscosity solutions are shown. Symbols indicate data for DNA of specific length: ■ = 11-mer, □ = 23-mer, ◊ = 35-mer, ○ = 47-mer. The spin-labeled DNAs are prepared as explained in the methods section and are measured at 9.2 GHz on a home-built time domain EPR spectrometer.[10,36] Sequences are shown in Table 1. The simulated values (solid line) are based on the calculated R_{1e} rates for a rigid rod with overall rotational correlation times that span the range of experimental values.[37] The measured rates are plotted as functions of the geometrically averaged rotational correlation time, $\bar{\tau} = \langle\tau_{\parallel}\tau_{\perp}^2\rangle^{1/3}$ for a rigid rod of the same dimensions as the DNA. Standard hydrodynamic theory is used to calculate the anisotropic rigid rod rotational correlation times as a function of length and viscosity.[72,73] In the bottom half of the figure, R_{1e} values for the four sequences, all in 0 w/v % sucrose, are shown. Error bars are shown with the data and are comparable in size to the markers. The markers are consistent for the different lengths, in both the top and the bottom sections of the figure.

theory[37] outlined in the Theory section, assuming that the DNA moves as a rigid object. It can be seen in Figure 2a that the theoretical prediction is about a factor of 2 smaller than the data. This discrepancy motivated this theoretical development to include the internal motions in the calculation of R_{1e} for DNA. Figure 2b illustrates that, as the length of the DNA increases, the R_{1e} drops up to ~35 base-pairs, but for 47 base-pairs, the R_{1e} has increased a statistically significant amount.

Figure 3 shows the spectral density functions as a function of the internal correlation time, using the L−S formulation of the spectral density function in eq 3.31. The uniform modes used for the rotational correlation times in the equation are those of the 23-mer, based on established hydrodynamic theory.[72,73] The spectral density functions are shown as a ratio to the spectral density for just the uniform modes, where $\mathbf{S}^2 = 1$. Figure 3 demonstrates that the internal motions can increase the spectral density functions as the order parameter is reduced, which becomes more pronounced as the internal correlation time approaches the reciprocal of the spectrometer frequency. Because the R_{1e} rates are proportional to the spectral density functions, then an increase in the spectral density function, as a result of including internal dynamics, will increase R_{1e}. This provides one possible qualitative explanation for why measured R_{1e} rates are higher than those predicted by only overall tumbling motions.

2. WBR Internal Dynamics Described by Stretched Exponential. We have mapped the WBR internal dynamics into a simple stretched exponential with an order parameter, $\mathbf{S}_p^2$, an internal correlation time, τ_p^I, and a stretched exponential power, β_p^I, as defined in eq 3.20. Figure 4 shows the effect of the

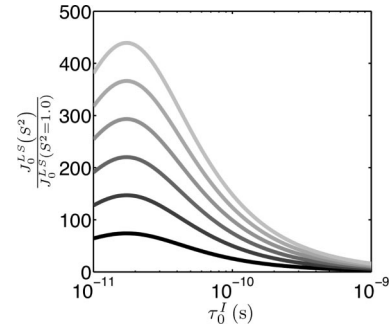

Figure 3. Lipari−Szabo spectral density for simple isotropic motion, $J_{p=0}^{LS} = \boldsymbol{R}\{\mathbf{S}^2(\tau_0/(1 + i\omega\tau_0)) + (1 - \mathbf{S}^2)(\tau^I/(1 + i\omega\tau^I + \tau^I/\tau_0))\}$, (eq 3.31) over a range of $\tau^I$and $\mathbf{S}^2$ values and for a spectrometer frequency of 9.2 GHz. The J_p^{LS} are shown relative to that of the spectral density from the uniform mode. The J_p^{LS} for each value of $\mathbf{S}^2$ is divided by the J_p^{LS} for the uniform modes, when $S^2 = 1$. The results are shown for $\mathbf{S}^2 = 0.9$ (black) through $\mathbf{S}^2 = 0.4$ (lightest grey). Diffusion coefficients for the overall molecule are calculated from hydrodynamic theory for rigid cylindrical models, based on the dimensions of a 23-mer duplex DNA at 21 °C and 1 cP.[72,73] The results for $p = 0$ are shown.

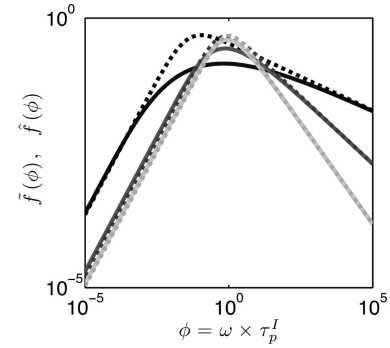

Figure 4. Stretched exponential spectral density times the spectrometer frequency, $\tilde{f}_{KWW}(\varphi) = \tau\tilde{f}_{KWW}(\omega)$ (solid lines) as given by eq 3.24, is plotted versus $\varphi = \omega\tau_p^I$ for different values of β. Overlaid (dash-dot lines) is the approximation given in eq 3.27, $\hat{f}(\varphi)$, which does very well in the limiting values away from the maximum. $\beta = 0.25$ is in black, $\beta = 0.75$ is in the lightest grey, and $\beta = 0.5$ is in between.

exponent β on the spectral density function eq 3.24: the smaller the exponential power β becomes, the larger the spectral density becomes at correlation times away from the peak center.

Figure 5 shows the dependence of $\mathbf{S}_p^2$, τ_p^I, and β_p^I on κ/kT, for a fixed twisting constant, $\alpha/kT = 100$, for a 23-mer DNA. κ/kT, a dimensionless quantity, can be directly interpreted as the number of base pairs in a persistence length. The range was chosen to span the ranges of persistence lengths reported in the literature. As κ/kT increases, $\mathbf{S}_p^2$ correspondingly increases for any value of p. Only bending modes contribute to the $p = 0$ case, which has the highest order. Figure 5a demonstrates that the order parameter increases as the bending force constant increase, which is consistent with the DNA becoming stiffer. In Figure 5b, τ_p^I decreases, as κ/kT increases for $p = 0, \pm1$. For the case where $p = \pm2$, τ_p^I does not change because the correlation function is dominated by the twisting dynamics, which are fixed by $\alpha/kT = 100$. The exponent β_p^I of the stretched exponential is roughly constant and around 1/2. It is somewhat larger for the $p = \pm2$ case because the twisting contribution is larger. It is not obvious why for the $p = \pm1$ case the exponent decreases.

Figure 6 shows $\mathbf{S}_p^2$, τ_p^I, and β_p^I as functions of the length of the DNA for two different values of κ/kT. The order parameter decreases monotonically with increasing length, and increases with increasing force constant. Comparing the $p = 0$ to the $p = \pm2$ case shows that the order parameter is less for the latter

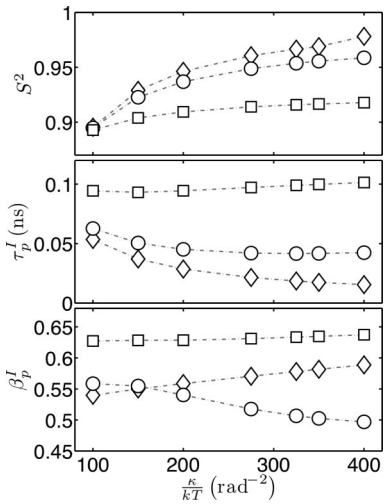

Figure 5. Order parameter, $\mathbf{S}_p^2$, and the parameters of the stretched exponential, τ_p^I, and β_p^I as a function of κ/kT and p, for a middle-labeled 23-mer DNA, using eq 3.14. The symbol □ represents $p = \pm 2$; ○ represents $p = \pm 1$, and ◊ represents $p = 0$. The stretched exponential is calculated from a least-squares fit to the site-specific WBR theory, using diffusion tensors for cylindrical molecules obtained from hydrodynamic theory, based on the dimensions of a 23-mer duplex DNA at 21 °C and 1 cP.[72,73] The $\mathbf{S}_p^2$ are calculated from the site-specific WBR model (3.18), as described within this work. The dotted lines are added only as an aid to the eye.

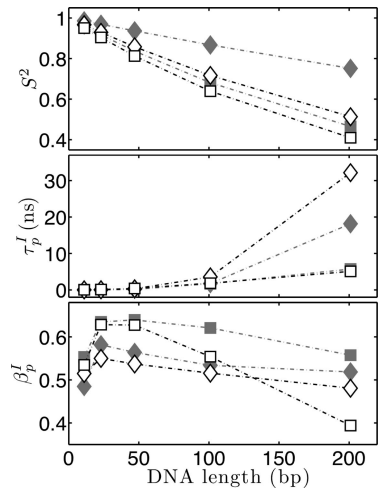

Figure 6. Order, $\mathbf{S}_p^2$, and stretched exponential parameters, τ_p^I, and β_p^I at $\kappa/kT = 150$ (white with black edges) and $\kappa/kT = 350$ (grey), for $p = 0$ (triangle, ▲) and $p = 2$ (squares, ■), for middle-labeled DNAs as a function of the length of the DNA, all at 21 °C and 1 cP. The length-dependent diffusion coefficients were calculated from the hydrodynamic theory for cylindrical molecules, based on the dimensions of duplex DNA.[72,73] The $\mathbf{S}_p^2$ are calculated from the site-specific WBR model (3.18). The dotted lines are added only as an aid to the eye.

case. This is expected, as the $p = \pm 2$ case includes the twisting dynamics, which reduces the order parameter. To a first approximation, the order parameter has an exponential dependence on $1/N$. In Figure 6b, τ_p^I increases with increasing length of the DNA, with a sharper increase for the $p = 0$ case. The value of τ_p^I is not affected by κ/kT when $p = 2$ because twisting is a dominant contribution. Figure 6c shows that β_p^I is near 1/2 for all lengths and bending rigidities and is maximal when the DNA is 25 to 50 base-pairs in length. The value of β_p^I drops most abruptly with length when $\kappa/kT = 150$, its less rigid value, and $p = 2$, as twisting has a higher contribution.

In Figure 7, we plot S_p^2, τ_p^I, and β_p^I as a function of the position along the DNA for a 23-mer. The order parameter decreases

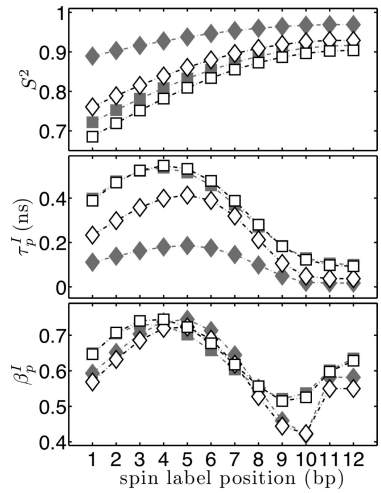

Figure 7. Parameters of a stretched exponential, $\mathbf{S}_p^2$, τ_p^I, and β_p^I, as a function of the position of the spin label on a 23-mer DNA at 21 °C and 1 cP. $\kappa/kT = 150$ (white with black edges) and $\kappa/kT = 350$ (grey), for $p = 0$ (triangles, ▲) and $p = \pm 2$ (squares, ■). The $\mathbf{S}_p^2$ are calculated from the site-specific WBR model (3.18). The base positions greater than 12 (not shown) are related to the ones less than 12 by mirror symmetry. The dotted lines are added only as an aid to the eye.

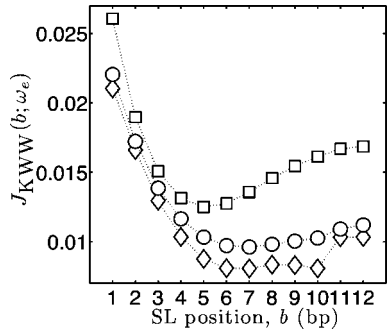

Figure 8. Stretched exponential-based spectral density function $J_p(\omega)$ (3.30) is plotted versus the position of the spin label and as a function of p, for a 23-mer DNA at 21 °C and 1 cP. The symbol □ represents $p = \pm 2$; ○ represents $p = \pm 1$, and ◊ represents $p = 0$. The parameters of a stretched exponential, S_p^2, τ_p^I, and β_p^I, for $\kappa/kT = 350$, are shown in Figure 7 and used in calculating $J_p(\omega)$.

monotonically toward the end of the DNA. The DNA is symmetric about the $b = 12$ base pair position. First order WBR theory shows that the order parameter at the end should be equal to the order parameter in the center raised to the fourth power. The internal correlation times are the largest at about 3/4 of the way toward the end. This is the position where the DNA is most flexible, where the first internal (the "horseshoe") mode is most active. As illustrated in Figure 4, as the DNA becomes stiffer as the internal correlation times become smaller.

Figure 8 shows a spectral density function that incorporates the results of the fitting of the stretched exponentials, for a spectrometer frequency of 9.2 GHz. Values of τ_p^I and β_p^I were obtained from fitting the position-dependent correlation functions for a 23-mer DNA. The spectral densities are highest at the ends of the 23-mer for all values of p. The spectral densities decrease sharply until $b \cong 6$, at which point they begin to increase again slightly. These spectral densities are frequency dependent and would be higher at a lower spectrometer frequency.

Discussion

The fundamental theory relates the relaxation rates for all mechanisms to spectral density functions. Figures 3 and 4

demonstrate the general features of the spectral density functions of stretched exponentials. They have their maximal value when the rates of motional processes, characterized as τ^{-1}, are on the order of the spectrometer frequency, or $\omega\tau \cong 1$. This holds for spectral densities that include internal motions (Figure 3) and spectral densities described by stretched exponentials (Figure 4). We suspect that the experimental R_{1e} rates decrease with increasing rotational correlation times (Figure 2a) because the relevant relaxation times are all larger than the optimal time, for which $\omega\tau = 1$. The spectral density functions for a DNA measured at 9.2 GHz are said to be in the "slow motional side" of the spectral density maximum.

Figure 3 provides insight into how the rates could increase as the length of the DNA increases (as noted in Figure 2b). The spectral densities increase when the internal correlation time is smaller ("shorter") than the uniform mode times and the order parameter decreases. If the internal correlation times were much faster than the spectrometer frequency, then as the order parameter decreased the spectral density would also decrease. Therefore, the numerical value of the internal time is extremely important in determining whether the spectral densities increase or decrease as the order parameter changes.

By equating the forms of internal relaxation predicted by the WBR model to those of the generalized spectral density functions, we can gain approximate insight into the WBR model's predictive capability to describe the proper internal correlation times and order parameters. Because the WBR model predicts order parameters and times for any positional correlation function, the full form and dependence on the index p can be kept in computing the spectral density functions. This is not possible with the model-free form, because there is no underlying structure to relate correlation functions with different indices. Figure 5 illustrates the dependence of the order parameters on the p index for different values of the bending force constant (with the twisting held constant). The parameters of the internal motion are plotted as a function of κ/kT because this (dimensionless) quantity is the number of discs contained in a persistence length. All of the order parameters increase as the bending constant increases, because the model of DNA is becoming stiffer. The $p = 0$ mode contains only the bending, and that term increases the most rapidly. The $p = \pm 2$ mode is most heavily weighted with the twisting and bending contributions muted in this term. Similar effects are seen in the internal correlation times, τ_p^I. Because twisting dominates the $p = \pm 2$ mode the time of that mode changes little. For the $p = 0$ mode, as the molecule becomes stiffer, the internal correlation times become smaller. This is a general feature of the WBR model for the motional modes for both twisting and bending. The values of the stretched exponent, β_p^I, really do not change much with stiffness, as they consistently are around 1/2, which was anticipated from the analytic theories of Schurr.[4,8] The surprising part is that for the $p = 0$ mode the exponent never goes below about 0.4, even though values as low as 1/4 have been suggested by theory; but such dependencies are only over limited time ranges. Therefore, the overall curves may be compromised by the early and late time regions where the correlation functions are simply exponential in time (i.e., not stretched), especially for short DNAs. Because $\beta_p^I \sim 1/2$, this underscores the need for a stretched exponential. As developed in Materials and Methods, the fit to a stretched exponential gave parameters that were accurate to a few percent, and an overall fit to the WBR correlation functions had a much smaller standard error than a single exponential. Further improvements to the fitting using two distinct stretched exponentials were minimal.

The dependence of the internal parameters on length is the one that bears most on the experimental observations (Figure 2). Figure 6 demonstrates that the order parameters, for all values of p, do indeed decrease with increasing length, when the bending and twisting force parameters are held constant. It is an assumption of the WBR model that the force parameters are indeed independent of length. For a larger κ/kT, the order drops more slowly as would be expected for a stiffer molecule. The decrease in order parameter with increasing length follows well the first order theory that the order parameters should decrease exponentially with increasing N.[8] The internal correlation times increase with length, in a fashion very similar to the increase in the correlation times of the normal modes, demonstrated previously.[21] The exponent, β_p^I, varies with N but within the 0.5−0.6 range.

An interesting test of the WBR model is the dependence on the position along the DNA. Figure 7 illustrates the dependencies for a 23 disk model. The order parameter decreases as the position of the label moves from the center to the end. Theory predicts that the order parameter at the ends should be equal to the order parameter in the middle raised to the fourth power.[21] This seems to be followed. The internal correlation times increase and are maximal about 1/4 of the way in. This is where the lowest internal eigenmode (the "horseshoe" shaped mode) is maximal. Because the DNA is so short, this mode can dominate the dynamics. This is affirmed by noticing that the exponent maximizes where the correlation times maximize, indicating that the decay curves are closer to single exponential, as though being dominated by a single mode. Figure 8 shows how the various terms (shown in Figure 7) contribute to the spectral density function. The spectral density is smallest in the center of the system and increases by about twofold toward the ends. This increase would be interpreted as greater flexibility of the ends. As one can see from the terms that contribute (Figures 7 and 8), the spectral density is a complicated mix of order parameter and correlation time. The shorter correlation time toward the end, coupled with the lower order parameter, allows the spectral density to increase. This demonstrates the principle that a site specific label can be a very good test of the internal dynamics.

Conclusions

We have shown that the correlation functions for the WBR model can be used to develop a formalism that parallels the L−S "model-free" approach. By adapting the L−S forms to include the WBR model, we provide a basis for relating order parameter and internal correlation time to the force constants of bending and twisting, as well as DNA length and position of spin label. In essence, we combine the simplicity of the model-free approach with the physically meaningful WBR model, which requires only two adjustable parameters.

Finally, to quantitatively understand the internal dynamics and simulate the spin−lattice relaxation rates of dsDNA, we have developed the correlation functions necessary to describe the spin rotation mechanism. This work represents the first attempt to include a many modes model into the velocity autocorrelation function, and the resulting forms should help explain the dependence of the spin rotation mechanism on internal dynamics. On the basis of the framework we have developed here, the R_{1e} for any given dsDNA can now be described on the basis of simply its overall tumbling rotational correlation times (which can be calculated rapidly on the basis of length, viscosity, and temperature), spectrometer frequency, spin label position within the dsDNA, and the two internal bending and twisting force constants, κ and α.

Acknowledgment. We thank Dr. J. M. Schurr for many helpful discussions. This work was supported in part by NIH GM65944, GM62360, and NIEHS P30ES07033, and the Iceland Research Fund (031490005, 60028021).

References and Notes

(1) Bloomfield, V. A.; Crothers, D. M.; Tinoco, I. Nucleic acids: structures, properties, and functions; University Science Books: Sausalito, CA, 2000.
(2) Wahl, P.; Paoletti, J.; Le Pecq, J.-B. *Proc. Natl. Acad. Sci. U.S.A.* **1970**, *65*, 417.
(3) Barkley, M. D.; Zimm, B. H. *J. Chem. Phys.* **1979**, *70*, 2991.
(4) Allison, S. A.; Schurr, J. M. *Chem. Phys.* **1979**, *41*, 35.
(5) Song, L. S.; Schurr, J. M. *Biopolymers* **1990**, *30*, 229.
(6) Thomas, J. C.; Allison, S. A.; Appellof, C. J.; Schurr, J. M. *Biophys. Chem.* **1980**, *12*, 177.
(7) Heath, P. J.; Clendenning, J. B.; Fujimoto, B. S.; Schurr, J. M. *J. Mol. Biol.* **1996**, *260*, 718.
(8) Schurr, J. M.; Fujimoto, B. S.; Wu, P.; Song, L. S. Fluorescence studies of nucleic acids: dynamics, rigidities, and structures. In *Topics in Fluorescence Spectroscopy*; Lakowicz, J. R., Ed.; Plenum Press: New York, 1992; pp 137.
(9) Wu, P.; Fujimoto, B. S.; Schurr, J. M. *Biopolymers* **1987**, *26*, 1463.
(10) Robinson, B. H.; Mailer, C.; Drobny, G. Site-specific dynamics in DNA: experiments. In *Annu. Rev. Biophys. Biomol. Struct.*; Stroud, R. M., Hubbell, W. L., Olson, W. K., Eds.; Annual Reviews Inc.: Palo Alto, 1997; Vol. 26, pp 629.
(11) Naimushin, A. N.; Fujimoto, B. S.; Schurr, J. M. *Biophys. J.* **2000**, *78*, 1498.
(12) Allison, S. A.; Austin, R.; Hogan, M. *J. Chem. Phys.* **1989**, *90*, 3843.
(13) Hagerman, P. J. *Annu. Rev. Biophys. Biophys. Chem.* **1988**, *17*, 265.
(14) Robinson, B. H. In *Stereodynamics of Molecular Systems*; Sarma, R. H., Ed.; Pergamon: New York, 1979.
(15) Robinson, B. H.; Forgacs, G.; Dalton, L. R.; Frisch, H. L. *J. Chem. Phys.* **1980**, *73*, 4688.
(16) Robinson, B. H.; Lerman, L. S.; Beth, A. H.; Frisch, H. L.; Dalton, L. R.; Auer, C. *J. Mol. Biol.* **1980**, *139*, 19.
(17) Spielmann, H. P.; Chi, D. Y.; Hunt, N. G.; Klein, M. P.; Hearst, J. E. *Biochemistry* **1995**, *34*, 14801.
(18) Strobel, O. K.; Kryak, D. D.; Bobst, E. V.; Bobst, A. M. *Bioconjug. Chem.* **1991**, *2*, 89.
(19) Hustedt, E. J.; Spaltenstein, A.; Kirschner, J. J.; Hopkins, P. B.; Robinson, B. H. *Biochemistry* **1993**, *32*, 1774.
(20) Miller, T. R.; Alley, S. C.; Reese, A. W.; Solomon, M. S.; McCallister, W. V.; Mailer, C.; Robinson, B. H.; Hopkins, P. B. *J. Am. Chem. Soc.* **1995**, *117*, 9377.
(21) Okonogi, T. M.; Reese, A. W.; Alley, S. C.; Hopkins, P. B.; Robinson, B. H. *Biophys. J.* **1999**, *77*, 3256.
(22) Keyes, R. S.; Bobst, A. M. *Biochemistry* **1995**, *34*, 9265.
(23) Strobel, O. K.; Keyes, R. S.; Sinden, R. R.; Bobst, A. M. *Biochemistry* **1995**, *324*, 357.
(24) Eimer, W.; Williamson, J. R.; Boxer, S. G.; Pecora, R. *Biochemistry* **1990**, *29*, 799.
(25) Alam, T. M.; Drobny, G. P. *Chem. Rev.* **1991**, *91*, 1545.
(26) Mattiello, D. L.; Drobny, G. P. Investigating furanose ring dynamics in oligonucleotides with solid state 2H NMR. In *NMR Probes of Molecular Dynamics*; Tycko, R., Ed.; Kluwer Academic Press: Amsterdam, 1994; pp 335.
(27) Nuutero, S.; Fujimoto, B. S.; Flynn, P. F.; Reid, B. R.; Ribeiro, N. S.; Schurr, J. M. *Biopolymers* **1994**, *34*, 463.
(28) Hustedt, E. J.; Kirschner, J. J.; Spaltenstein, A.; Hopkins, P. B.; Robinson, B. H. *Biochemistry* **1995**, *34*, 4369.
(29) Barhate, N.; Cekan, P.; Massey, A. P.; Sigurdsson, S. T. *Angew. Chem., Int. Ed.* **2007**, *46*, 2655.
(30) Freed, J. H. Theory of slow tumbling ESR spectra for nitroxides. In *Spin Labeling: Theory and Applications*; Berliner, L. J., Ed.; Academic Press: New York, 1976; pp 53.
(31) Hustedt, E. J.; Cobb, C. E.; Beth, A. H.; Beechem, J. M. *Biophys. J.* **1993**, *64*, 614.
(32) Okonogi, T. M.; Alley, S. C.; Reese, A. W.; Hopkins, P. B.; Robinson, B. H. *Biophys. J.* **2000**, *78*, 2560.
(33) Okonogi, T. M.; Alley, S. C.; Reese, A. W.; Hopkins, P. B.; Robinson, B. H. *Biophys. J.* **2002**, *83*, 3446.
(34) Robinson, B. H.; Drobny, G. P. Site-specific dynamics in DNA: theory and experiment. In *Methods in Enzymology*; James, T. L., Ed.; Academic Press: San Diego, 1995; Vol. 261, pp 451.
(35) Robinson, B. H.; Drobny, G. P. Site-specific dynamics in DNA: theory. In *Annu. Rev. Biophys. Biomol. Struct.*; Stroud, R. M. , Hubbell, W. L. , Olson, W. K. , Eds.; Annual Reviews Inc.: Palo Alto, 1995; Vol. 24, pp 523.
(36) Nielsen, R.; Canaan, S.; Gladden, J. A.; Gelb, M. H.; Robinson, B. H. *J. Magn. Reson.* **2004**, *169*, 129.
(37) Mailer, C.; Nielsen, R.; Robinson, B. H. *J. Phys. Chem. A* **2005**, *109*, 4049.
(38) Hyde, J. S.; Dalton, L. R. Saturation-transfer spectroscopy. In *Spin Labeling*; Berliner, L. J. , Eds.; Academic Press, Inc.: New York, 1979; Vol. II.
(39) Altenbach, C.; Froncisz, W.; Hyde, J. S.; Hubbell, W. L. *Biophys. J.* **1989**, *56*, 1183.
(40) Froncisz, W.; Hyde, J. S. *J. Magn. Reson.* **1982**, *47*, 515.
(41) Huisjen, M.; Hyde, J. S. *Rev. Sci. Instrum.* **1974**, *45*, 669.
(42) Hyde, J. S.; Yin, J. J.; Feix, J. B.; Hubbell, W. L. *Pure Appl. Chem.* **1990**, *62*, 255.
(43) Subczynski, W. K.; Hyde, J. S.; Kusumi, A. *Proc. Natl. Acad. Sci. U.S.A.* **1989**, *86*, 4474.
(44) Nielsen, R.; Che, K.; Gelb, M. H.; Robinson, B. H. *J. Am. Chem. Soc.* **2005**, *127*, 6430.
(45) Columbus, L.; Hubbell, W. L. *Trends Biochem. Sci.* **2002**, *27*, 288.
(46) Thomas, D. D.; Seidel, J. C.; Gergely, J.; Hyde, J. S. *J. Supramol. Struct.* **1975**, *3*, 376.
(47) Lipari, G.; Szabo, A. *Biochemistry* **1981**, *20*, 6250.
(48) Lipari, G.; Szabo, A. *J. Am. Chem. Soc.* **1982**, *104*, 4546.
(49) Lipari, G.; Szabo, A. *J. Am. Chem. Soc.* **1982**, *104*, 4559.
(50) Schurr, J. M.; Babcock, H. P.; Fujimoto, B. S. *J. Magn. Reson. B* **1994**, *105*, 211.
(51) Qin, P. Z.; Dieckmann, T. *Curr. Opin. Struct. Biol.* **2004**, *14*, 350.
(52) Song, L. S.; Allison, S. A.; Schurr, J. M. *Biopolymers* **1990**, *29*, 1773.
(53) Alvarez, F.; Alegria, A.; Colmenero, J. *Phys. Rev. B* **1991**, *44*, 7306.
(54) Bergman, R. *J. Appl. Phys.* **2000**, *88*, 1356.
(55) Lindsey, C. P.; Patterson, G. D. *J. Chem. Phys.* **1980**, *73*, 3348.
(56) Provencher, S. W. *J. Chem. Phys.* **1976**, *64*, 2772.
(57) Svanberg, C. *J. Appl. Phys.* **2003**, *94*, 4191.
(58) Robinson, B. H.; Reese, A. W.; Gibbons, E.; Mailer, C. *J. Phys. Chem. B* **1999**, *103*, 5881.
(59) Abragam, A. *The Principles of Nuclear Magnetism*; Clarendon Press: Oxford, 1961.
(60) Hubbard, P. S. *Phys. Rev. A* **1974**, 9.
(61) Hubbard, P. S. *Phys. Rev. A* **1977**, 15.
(62) McClung, R. E. D. *J. Chem. Phys.* **1980**, 73.
(63) Hubbard, P. S. *Phys. Rev. A* **1973**, 8.
(64) Atkins, P. W.; Kivelson, D. *J. Chem. Phys.* **1966**, *44*, 169.
(65) Torrey, H. C. *Phys. Rev.* **1953**, *92*, 962.
(66) Robinson, B. H.; Haas, D. A.; Mailer, C. *Science* **1994**, *263*, 490.
(67) de Gennes, P.-G. *J. Phys. Chem. Solids* **1958**, *7*, 345.
(68) Schurr, J. M. *J. Chem. Phys.* **1984**, *84*, 71.
(69) Zwanzig, R. *Nonequilibrium statistical mechanics*; Oxford University Press: New York, 2001.
(70) Hubbard, P. S. *Phys. Rev.* **1963**, 131.
(71) Okonogi, T. M. *Dynamics, thermodynamics, and structural investigations of nucleic acids using site-specific spin-labeling and electron paramagnetic resonance*; University of Washington, 2000.
(72) Tirado, M. M.; Torre, J. G. d. l. *J. Chem. Phys.* **1979**, *71*, 2581.
(73) Tirado, M. M.; Torre, J. G. d. l. *J. Chem. Phys.* **1980**, *73*, 1986.
(74) Schurr, J. M.; Fujimoto, B. S.; Nuutero, S. *J. Magn. Reson.* **1994**, *106*, 1.
(75) Rangel, D. P.; Sucato, C. A.; Spink, C. H.; Fujimoto, B. S.; Schurr, J. M. *Biopolymers* **2004**, *75*, 291.
(76) Barber, E. J. *National Cancer Institute monograph* **1966**, *21*, 219.
(77) Fujimoto, B. S.; Schurr, J. M. *Nature* **1990**, *344*, 4055.

JP7111704